June 07, 2023

Study of vector control strategy on Interior Permanent Magnet Synchronous Motors

Prabhu Bernard

MASTER'S THESIS
Degree Project in Electric Vehicle Technology (EXE700)
Department of Engineering Science

Preface

This thesis was performed as part of the 'Electric Vehicle Engineering' Master program at University West in Trollhättan, Sweden. It is a study spanning ten weeks, equivalent to accruing 15 academic credits at the university level. As a Driveline Engineer at Epiroc Rock Drills AB, a Swedish mining and infrastructure equipment manufacturer, my work is centered around the research and development of battery powered mining vehicles. The focus of driveline development at Epiroc is to devise functions that ensure safety, precise control, and maneuverability of vehicles within mining environment that often weighs more than 40 tons.

The inspiration for the thesis originated from a desire to understand the intricate operations of an electric motor and how motor control strategy could be optimized for motor efficiency. Research aimed to understand the advantages and drawbacks of direct torque control, and to uncover the possibilities of performance enhancement. To accomplish this, a blend of theoretical analysis and simulation-based study was conducted. Illustrations in this report that are not attributed to other sources has been created by the author.

I am profoundly thankful to my academic advisor, Mr. Niklas Hansson, for his invaluable counsel and insight throughout this thesis, and to my manager and advisor at Epiroc, Mr. Jens Eriksson, for his motivation and guidance throughout this master program. Without their wisdom and patience, this project would not have been possible. Above all, the unwavering support from my wife has been indispensable in this endeavor.

Trollhättan, June 2023

Prabhu Bernard

Abstract

This thesis presents a comprehensive study of Direct Torque Control (DTC) for Interior Permanent Magnet Synchronous Motors (IPMSMs) evaluating its potential in high performance motor drive systems. The research begins with a literature review, looking into the fundamental principles of DTC, Pulse Width Modulation (PWM), Space Vector Modulation (SVM) and Field Oriented Control (FOC).

The methodology section involves the detailed modeling of IPMSM using Simulink for a precise representation of system dynamics. The Park and Clarke transformations are employed in the phase transformation of currents and voltages to simplify the control strategy. The implementation of Voltage Source Inverter (VSI) is explored and its crucial role in modulating input signals is discussed. Subsequently, the implementation of DTC is demonstrated, capturing the key focus of the thesis.

The validation stage verifies the model created in Simulink against research papers published in the same field. This is coupled with an analysis of sector selection and switching table in enhancing DTC performance. The results and conclusion reassess the voltage and flux vectors, evaluating their influence on the system. Additionally, the effectiveness of Proportional-Integral (PI) control for maintaining the desired speed and torque is analyzed.

Thus, this thesis offers a holistic perspective on the implementation and performance of DTC for IPMSMs, contributing to the existing body of knowledge and paving the way for future research in this field.

Date:	June 07, 2023
Author(s):	Prabhu Bernard
Examiner:	Lena Max
Advisor(s):	Niklas Hansson (University West), Jens Eriksson (Epiroc Rock Drills AB)
Programme name:	Degree Project in Electric Vehicle Technology (EXE700)
Main field of study:	Electric Vehicle Technology
Course credits:	15 HE credits.
Publisher:	University West, Department of Engineering Science, S-461 86 Trollhättan, SWEDEN

Contents

Figures

Tables

Nomenclature

Glossary

DTC	=	Direct Torque Control
PMSM	=	Permanent Magnet Synchronous Motor
FOC	=	Field Oriented Control
MPC	=	Model Predictive Control
SVM	=	Space Vector Modulation
EV	=	Electric Vehicle
IM	=	Induction Motor
PWM	=	Pulse Width Modulation
DSC	=	Direct Self Control
DC	=	Direct Current
IPMSM	=	Internal Permanent Magnet Synchronous Motor
IGBT	=	Insulated Gate Bipolar Transistors

1 Introduction

In an era where motor control methodologies are rapidly evolving, fueled by a surging demand for energy efficient and high-performance electric vehicles, Direct Torque Control (DTC) still stands out as a valuable technique for controlling Permanent Magnet Synchronous Motors (PMSMs). From its inception in the mid-1980s, DTC has gained significant attention in the field of motor control due to its ability to provide faster torque and flux control at the expense of higher torque ripple when compared to traditional control strategies like Field Oriented Control (FOC). However, DTC has undergone significant evolution over the years by combining other control methods such as Model Predictive Control (MPC) and Space Vector Modulation (SVM) to further optimize the performance and minimize torque ripple.

PMSMs have become increasingly popular due to their high efficiency, compact design, and sturdy operation. In comparison to other motors, PMSMs have a high torque-to-weight ratio, wide operating speed range, and low maintenance requirements [1]. This makes them ideal for electric vehicles. Consequently, the development of optimal control methodologies, such as DTC and FOC, has become essential to ensure the best performance and efficiency in EV applications. Originally designed for Induction Motors (IM), researchers have adapted DTC for PMSMs. The primary difference between the two motor types is the presence of permanent magnets in PMSMs which creates a direct axis (d-axis) magnetic field that affects the stator flux linkage and electromagnetic torque of the motor. PMSM also require advanced observer methods to accurately estimate the torque and flux.

This thesis mainly focuses on the study of DTC for Interior Permanent Magnet Synchronous Motors (IPMSMs), looking into its underlying principles, benefits, and limitations. To better understand DTC and how it works in practice, the thesis includes a comprehensive simulation study to analyze the behavior and provide valuable insights into its performance. The simulation results are then validated against a peer reviewed research within the same field. Although DTC and FOC have similarities, DTC has some unique advantages. Both techniques aim to reduce torque and flux ripple, but DTC directly calculates and controls torque and stator flux, avoiding the need for pulse width modulation (PWM) and coordinate transformations.

In this context, it is crucial to understand the dynamic interaction between the motor and control system that is deeply intertwined with the strategy applied. Making this a finely balanced act of optimization. The comprehensive study, combined with simulation and cross-validation with peer reviewed research aims to demystify the complexities of DTC. The unique capability of the control method to offer quick torque and flux control – a property that is well known since its inception continues to be a vital part of motor control. As the landscape of motor control systems and electric vehicles continue to evolve, the importance of understanding and effectively leveraging the benefits of this control strategy cannot be overstated. This thesis hopes to offer a deeper understanding of this crucial control technique while discussing its benefits and limitations.

2 Literature Review

From traditional scalar control to advanced DTC, motor control strategies remain as an ever evolving and significant field of research that caters to various industries and applications. A few of the key concepts and strategies that contributed to the field of motor control are discussed in this session.

2.1 Open and Closed loop system

Open and closed loop control systems both aim to regulate processes and maintain stability of a system as presented in [Figure 2.1]. Open loop systems solely rely on predetermined input-output relations that are relatively simple and cost effective. They are commonly used in household appliances like microwaves and washing machines. Their inability to adapt to dynamic conditions and disturbances in the system limit their effectiveness. Instead, closed loop system constantly monitors and changes the outputs based on sensor feedback received from the actual state of the system. By comparing the output with a desired setpoint or reference value, closed loop systems can identify and correct errors in real time. This results in greater precision, adaptability, and robustness of the system, making them ideal for dynamic applications like advanced motor control techniques and robotics.

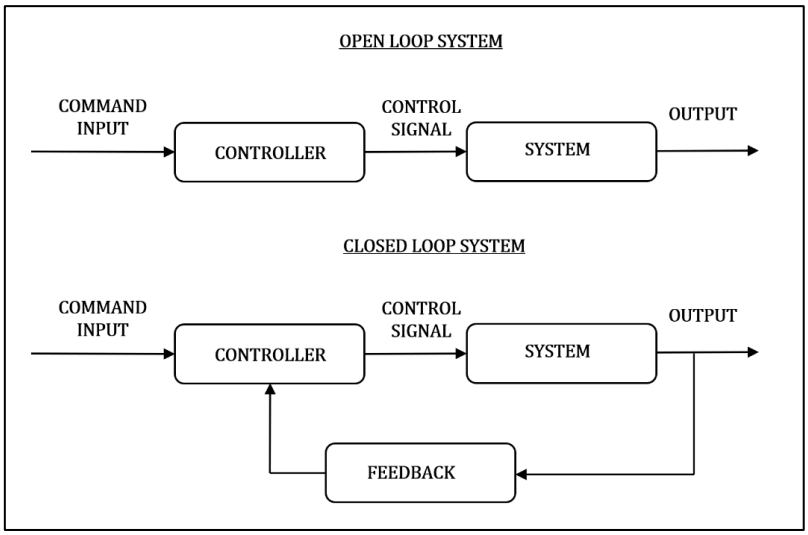

Figure 2.1 Open and Closed loop system

When it comes to voltage regulators, current regulators, hysteresis controllers and space vector modulators, the feedback loop of the control system plays an important role. In case of voltage controllers, errors will arise because of propagation of logic delays, switching deadtime and voltage drop across semiconductors. Whereas in current controllers, even with an ideal inverter, there will still be a deviation between the actual and setpoint current that will have a net effect on the output that causes deviations in the average q- and d-axis currents. Feedback loop ensures that the desired functionality is precisely achieved [2].

2.2 Direct Torque Control

DTC was first introduced in an IEEJ research paper published by I. Takahashi and T. Noguchi in 1984 as a new control strategy for IM. It was later published in an IEEE paper in 1986 [3]. Meanwhile the concept was patented by M. Depenbrock as Direct Self Control (DSC) in the year 1985 in Germany. The technique quickly gained a significant attention within the scientific community owing to its simplicity, good performance, and robustness. The possibility of obtaining a good dynamic torque control without a mechanical transducer on the motor shaft categorized this into a "sensorless type" control [4]. A block diagram representing the classic DTC control is presented in [Figure 2.2] which provides an overview of DTC logic. It starts with measuring the voltage and current that is transformed to simpler two-phase system using Clark transformation. These measurements are used to estimate the stator torque and flux, which are compared with their reference values. The resulting differences are processed in a hysteresis controller, which helps in selecting the appropriate voltage vectors. This volage vector is then converter to required AC voltage form through a voltage source inverter, allowing efficient and precise control of motor torque and flux. A comprehensive study into the underlying logic of DTC is presented in [Chapter 3.4]

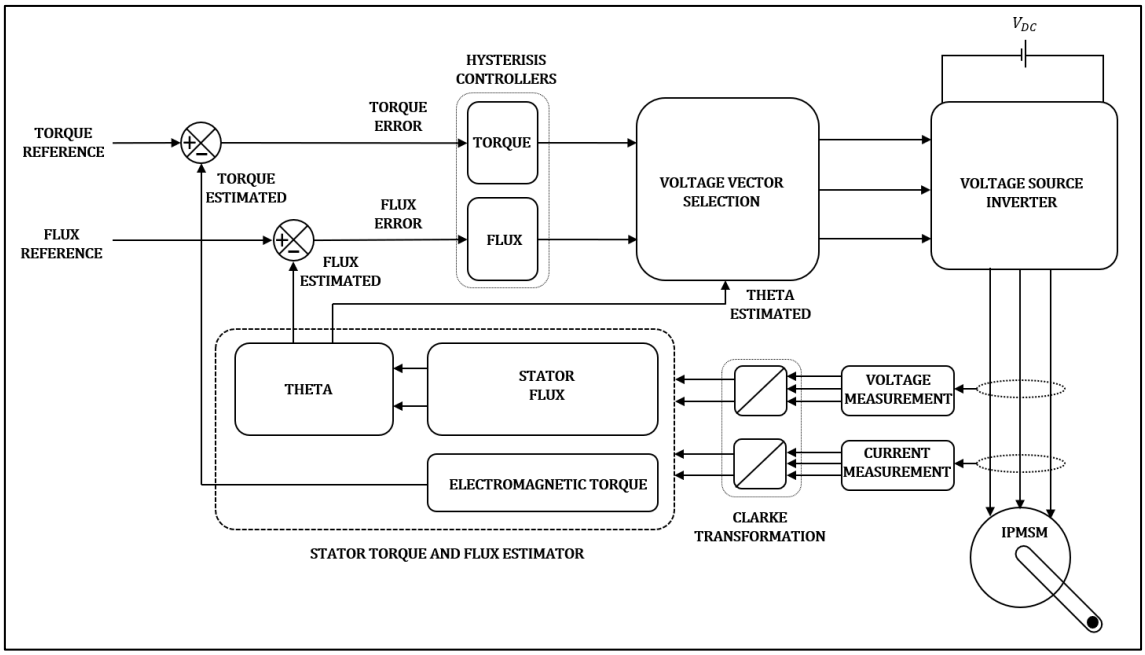

Figure 2.2 Overview of Direct Torque Control

It is possible to directly control the switching states of an inverter to keep the torque and flux errors within a predefined hysteresis band limit. This technique was further developed to work with different motor topologies like PMSM over the years. DTC also presented a fair share of disadvantages when compared to other techniques. The torque and the flux were difficult to control at low speeds which also resulted in increased noise levels at those speeds. It also showcased a variable switching frequency behavior. This classic method was also known for its high current and torque ripples during operation.

In recent years, several researchers have tried to address the drawbacks of the DTC method and the solutions were focused on improvements in the switching table, introducing SVM techniques to reduce torque ripple and developing more complex solutions dealing with fuzzy logic and neural networks [4]. However, this took away the key feature of simplicity from the control strategy.

2.3 Pulse Width Modulation

Pulse width modulation (PWM) is a modulation technique used in many digital and analogue circuits. A typical PWM-based system uses a set switching frequency and modulates the width of the pulses to control the voltage and frequency of the motor. At the heart of the PWM lies the comparison between a reference waveform and a carrier waveform. The reference waveform, typically sinusoidal in nature, represents the desired output voltage. The carrier waveform, typically triangular or sawtooth in nature, serves as a modulation index (ratio of the amplitude of reference waveform to the amplitude of carrier waveform). This results in a modulated signal with varying pulse widths, which is then passed through a low pass filter to recover the desired output waveform. Two of the commonly used PWM techniques are Sinusoidal PWM and Space vector PWM [5]. Space vector PWM is the method that is used in the DTC control of IPMSMs. An illustration of sinusoidal PWM wave is presented in [Figure 4.3].

2.4 Space Vector Modulation

The concept of SVM gained popularity in the 1990s, whereas the integration of SVM into DTC emerged in the early 2000s. Integration of both techniques further enhanced the overall performance of the electric drives. SVM is a PWM technique that manipulates the switching states of inverters by using a space vector representation. It ensures an optimum use of DC bus voltage and minimizes the harmonic distortions that arise in the output voltage wave form. This results in a significant torque ripple reduction and efficiency improvement for the motor. Instead of a switching table, a voltage modulator is utilized. The predictive controller determines the stator voltage command vector in polar co-ordinates which generates the switching pulses S_A, S_B, S_C to control the inverter [1]. Despite the lower switching frequency, this guarantees lower current and torque ripples due to the SVM operation. In contrast to the hysteresis operation, inverter switching in SVM is unipolar with reduced harmonic distortions.

SVM uses the switch on time per sector for voltage modulation. [Figure 2.3] shows a brief overview of SVM for a voltage vector (marked red) in a sector (marked grey). The angular position of the vector is controlled by only switching between basic vectors $(V_3 \,\&\, V_4)$ whereas the magnitude of the of the vector is controlled by switching between basic vectors $(V_3 \,\&\, V_4)$ along with null vectors $(V_0 \,\&\, V_7)$. The duration of the switching is important for a smooth rotation of the voltage vector. For example, if the voltage vector is closer to (V_3) then the duration of switch on-time of (V_3) is more than that of (V_4).

In Classical DTC, the voltage vector is selected based on a switching table as discussed in [Chapter 3.6] instead of considering the switching time of the vector in each sector. SVM allows a constant switching frequency, and the shape of the modulation waveform fully utilizes the DC source voltage which makes it more efficient. The main difference between the switching table selection and SVM lie in the complexity of harmonic distortions of the output.

Researchers have combined these two methods to create DTC-SVM that provides fast response of DTC and good harmonic performance of SVM [1].

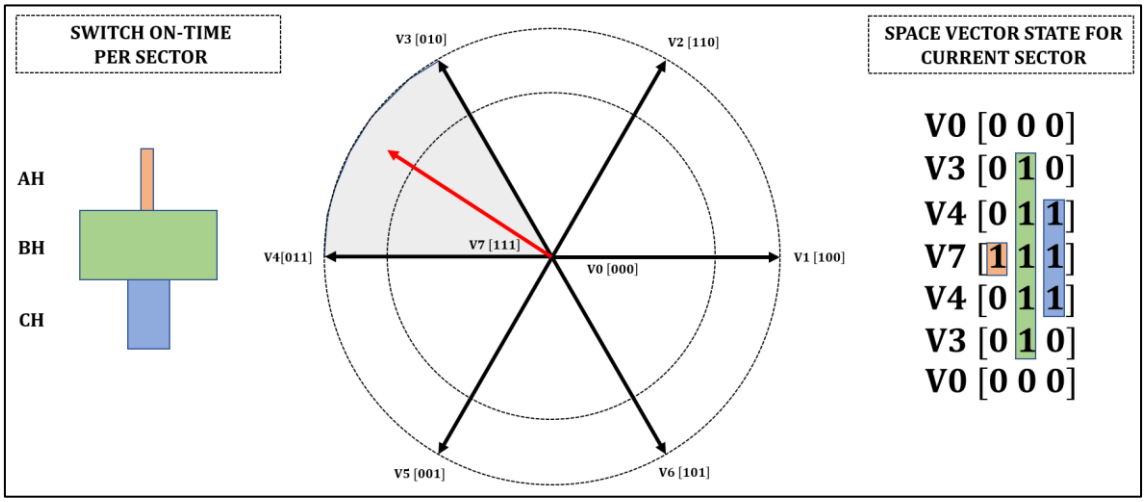

Figure 2.3 Overview of Space Vector Modulation

2.5 Field Oriented Control

FOC was first introduced in a research paper published in an IFAC conference by F. Blaschke in 1971. The control strategy was primarily developed to improve the dynamic performance of the IM by achieving a separate control of torque and flux commonly referred to as "decoupling". The two parameters were decoupled by aligning the stator current vector with the rotor magnetic field. An overview of FOC is presented in [Figure 2.4].

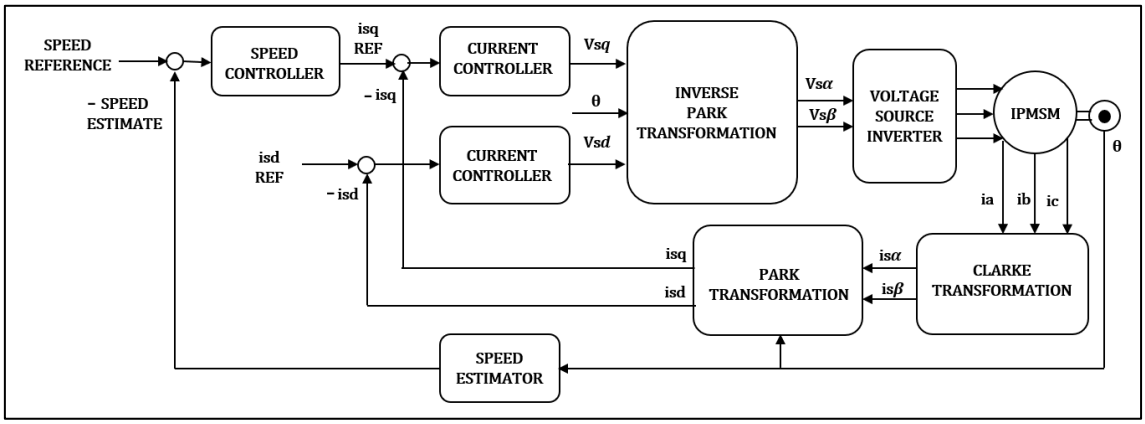

Figure 2.4 Overview of Field Oriented Control

Once the stator currents are in the synchronous reference frame, FOC manages the torque and flux components separately. Typically, a current controller is used to regulate the reference values of both the torque and flux. This transformed the behavior of an IM to resemble that of a separately excited DC motor which allows a precise control of torque and speed [4].

The main idea behind FOC is to simplify the relationship between stator current and rotor magnetic field by controlling the stator currents. This is done by transforming the 3-phse stator currents into a two-dimensional coordinate system $(d-q)$ axis that rotates as the same speed as the rotor. In this coordinate system, the $(d-axis)$ current (i_d) aligns with the rotors magnetic field, while the $(q-axis)$ current (i_q) is 90° out of phase. The torque produced by the motor can be controlled by the $(q-axis)$ current while magnetic flux can be controlled by the $(d-axis)$ current. This decoupling of the torque and flux allows a precise and efficient control of the motor. The $(d-q)$ currents cannot be directly controlled since they are mathematical transformations of actual stator currents. Hence a process of inverse Park transformation is used to covert the $(d-q)$ currents back into 3-phase currents. In addition to that, FOC requires the rotor position (θ) obtained by a sensor for proper implementation.

2.6 Clarke and Park Transformation

The decoupling of the torque and flux in the FOC control discussed in [Chapter 2.5] involves a series of coordinate transformations called Clarke and Park transformation as presented in [Figure 2.5].

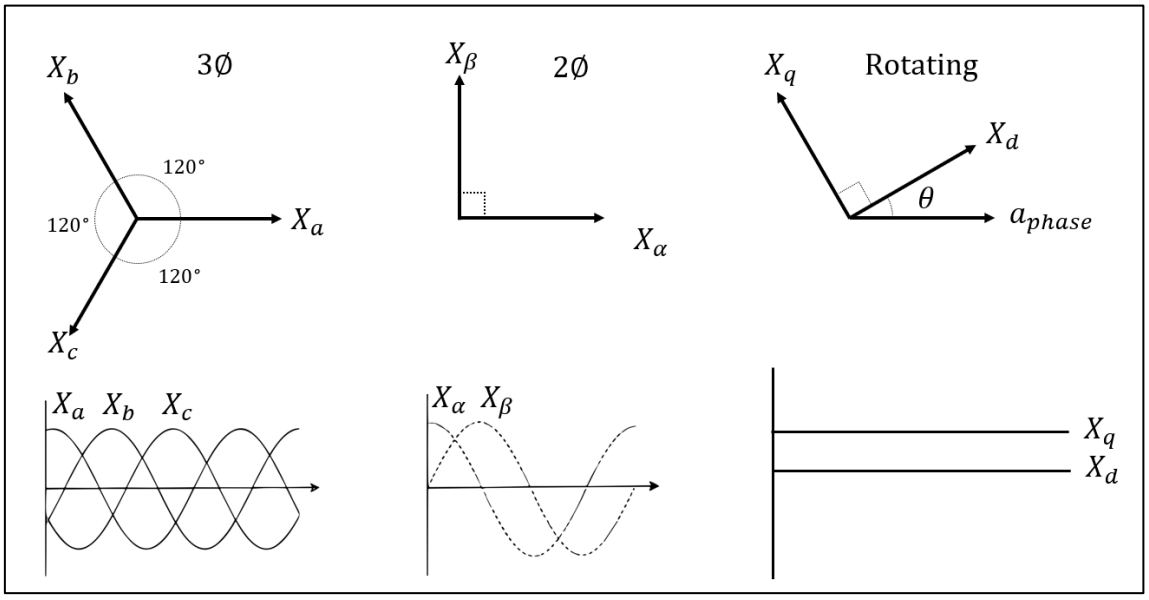

Figure 2.5 Clarke and Park Transformation

Clarke transformation, also known as $(\alpha-\beta)$ transformation, converts the 3-phase stator currents into equivalent 2-phase stationary reference frame. The transformation results

in two orthogonal components (α) and (β), representing the stator currents which retains the power and torque information that enables further processing. Park transformation, or the $(d-q)$ transformation, shifts these 2-phase currents into a rotating reference frame, called synchronous reference frame or the $(d-q)$ frame

This frame that rotates at the same speed as the rotor magnetic field makes the control of stator currents simpler. This uses the information about the rotor position (θ) to perform the coordinate transformation. The d-component corresponds to the magnetizing current, and the q-component corresponds to the torque producing current. Upon the completion of the control process that determines the stator voltages and currents in the $(d-q)$ frame, an inverse Park transformation to convert back to $(\alpha-\beta)$ frame followed by an inverse Clarke transformation to retrieve the 3 phase voltages (or currents) are applied. Finally, the PWM is applied to generate the voltage waveforms. A detailed illustration of this process is presented in [6].

2.7 PMSM modeling and simulation

Permanent Magnet Synchronous Motor (PMSM) is a popular choice for applications that require high efficiency and power density. Increasing demand for electric vehicles has accelerated the need for advanced PMSM modeling and control techniques. Based on the orientation of the magnetic field with respect to the axis of rotation, PMSMs are generally classified into radial and axial flux machines. The selected motor for this thesis has radial flux with interior mounted permanent magnets intended for high-speed applications. A major consequence that arises with the mounting of permenant magnet is the difference in the direct and quadrature axis inductance values [7]. The motor control strategies discussed in the preceding sub chapter has its own advantages and disadvantages. Simulation tools like MATLAB and Simulink are often used to examine the behavior of different control methods.

Simulations enable researchers to iterate through various designs, algorithms and configurations efficiently thereby accelerating the development process. Rapid prototyping along with parameter sensitivity analysis assists in identifying the critical parameters and facilitates optimization. This also ensures a safe environment for learning, testing, and validating control algorithms. The shortcomings and trade-offs of the control strategies DTC, FOC and DTC-SVM implemented in PMSM drives are studied with the help of simulation tools and an overview is presented in [8]. DTC offers high dynamic torque response and simpler construction at the expense of higher acoustic noise and torque ripple. FOC is more complex due to coordinate transformations while providing a precise controls and better performance with low torque ripple. However, it requires current and rotor position sensors. On the other hand, DTC-SVM combines the benefits of both, providing high dynamic response of DTC and low torque ripple of FOC. It also offers better performance at low speeds than traditional DTC.

The ideas explored in this chapter serve as a foundational basis for the entirety of the research conducted in this thesis.

3 Methodology

3.1 Mathematical model of IPMSM

To simplify the analysis and control of synchronous machines, a mathematical process is used to transform the sinusoidal 3-phase system into an equivalent 2-axis co-ordinate system that rotates synchronously with the rotor's magnetic field. This transformation of 3-phase stator currents (or voltages) to the direct axis and quadrature axis components is known as Park transformation.

The d-axis (direct axis) is aligned with the rotor's magnetic field. It represents the component of the stator current that generates magnetic flux in the same direction as the rotor's magnetic field. The d-axis current is attributed to handle the magnetic flux of the motor. It is often recommended to keep it as low as possible for optimum efficiency. Whereas q-axis (quadrature axis) is perpendicular to the d-axis and consequently, to the rotor's magnetic field. It represents the component of the stator current that generates a magnetic field perpendicular to the rotor's magnetic field as presented in [Figure 3.1]. For PMSM, the q-axis current is responsible for generating torque in the motor. The motor control system's aim is to optimize the q-axis current to achieve maximum torque.

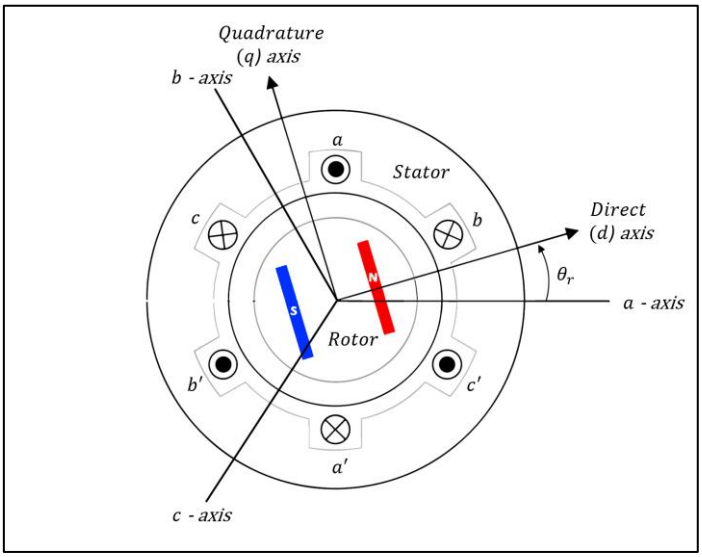

Figure 3.1 3-phase 2 pole IPMSM d-axis and q-axis

The mathematical model of an IPMSM developed with Simulink facilitates the study of torque and flux characteristics. A generic model can be derived from the vector quantities illustrated in different coordinate axes as shown in [Figure 3.2]. Two rotating reference frames are presented as $(x-y)$ and $(d-q)$ whereas the stationary reference frame is presented as $(\alpha-\beta)$. The stator flux linkage (φ_s) is aligned with the $(x-axis)$ and the rotor flux linkage (φ_r) is aligned with the $(d-axis)$. (θ_s) and (θ_r) are the respective angles. The stator equations (3.1) and (3.2) in the rotor reference frame using flux linkages describes the dynamic behavior of the motor [7].

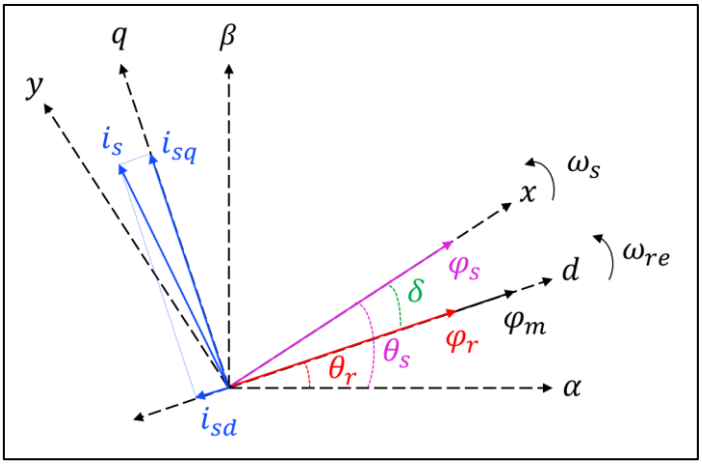

Figure 3.2 IPMSM Phasor diagram

$$V_{sd} = R_s i_{sd} + \frac{d}{dt}(\varphi_{sd}) - \omega_{re}\varphi_{sq} \tag{3.1}$$

$$V_{sq} = R_s i_{sq} + \frac{d}{dt}(\varphi_{sq}) + \omega_{re}\varphi_{sd} \tag{3.2}$$

$$\varphi_{sd} = L_d i_{sd} + \varphi_m \tag{3.3}$$

$$\varphi_{sq} = L_q i_{sq} \tag{3.4}$$

$$T_e = \frac{3}{2}\frac{p}{2}(\varphi_{sd} i_{sq} - \varphi_{sq} i_{sd}) \tag{3.5}$$

Stator flux linkage in $d-q$ reference frame from [Figure 3.2] can also be written as

$$\varphi_{sd} = \varphi_s \cos\delta \tag{3.6}$$

$$\varphi_{sq} = \varphi_s \sin\delta \tag{3.7}$$

Where:

V_{sd}, V_{sq}	Stator voltages in the $d-q$ reference frame
i_{sd}, i_{sq}	Stator currents in the $d-q$ reference frame
$\varphi_{sd}, \varphi_{sq}$	Stator flux linkage in the $d-q$ reference frame
L_d, L_q	Stator inductances in the $d-q$ reference frame
R_s	Stator resistance
φ_m	Permanent magnet flux linkage
T_e	Electromagnetic torque in terms of stator flux and current
ω_s, ω_{re}	Angular velocity of the stator and rotor
δ	Load / torque angle between the rotating stator and rotor flux
p	Number of poles of the magnet

The stator flux aligned with the x-axis $(\varphi_{sx} = \varphi_s, \varphi_{sy} = 0)$. It is important to note that stator flux along the y-axis is assumed to be zero to simplify the control algorithm. Imperfections in the motor, controller and measurements typically result in stator flux components appearing along the y-axis. Nevertheless, these components are generally minor and can be ignored in majority of practical situations.

By substituting the equations (3.3) and (3.4) into (3.5), the electromagnetic torque can be rewritten as

$$T_e = \frac{3}{2}\frac{p}{2}\left(\left(L_d - L_q\right)i_{sd}i_{sq} + \varphi_m i_{sq}\right) \tag{3.8}$$

The primary distinction between the surface mounted PMSM and IPMSM is the presence of reluctance torque in the latter. In surface mounted PMSM, the direct and quadrature axis inductances are the same. i.e., $L_d = L_q$. Whereas in IPMSM due to the asymmetry in flux path inductances are different, i.e., $L_q > L_d$. The presence of reluctance torque increases the power density of the motor. The relation between the load torque and the electromagnetic torque defines the dynamic behavior of the motor, commonly known as "swing equation" [5]. In practical applications a viscous damping coefficient "B" is added to this relation to account for the frictional losses in the system.

$$T_e - T_m = J\frac{d}{dt}(\omega_m) + B\omega_m \tag{3.9}$$

Where:

T_m	Load Torque
J	Motor Inertia
ω_m	Mechanical Speed of the rotor shaft
B	Viscous damping coefficient

By substituting equations (3.3) and (3.4) into (3.1) and (3.2), the stator voltages in the $d-q$ reference frame can be rewritten as

$$V_{sd} = R_s i_{sd} + \frac{d}{dt}(L_d i_{sd} + \varphi_m) - \omega_{re} L_q i_{sq} \tag{3.10}$$

$$V_{sq} = R_s i_{sq} + \frac{d}{dt}\left(L_q i_{sq}\right) - \omega_{re}(L_d i_{sd} + \varphi_m) \tag{3.11}$$

By using the equations (3.10) and (3.11) stator currents in the $d-q$ reference frame can be derived.

$$i_{sd} = \int \frac{1}{L_d}\left(V_{sd} - R_s i_{sd} + \omega_{re} L_q i_{sq}\right) \tag{3.12}$$

$$i_{sq} = \int \frac{1}{L_q}\left(V_{sq} - R_s i_{sq} - \omega_{re}(L_d i_{sd} + \varphi_m)\right) \tag{3.13}$$

By using the equations (3.9), mechanical speed of the rotor can be derived.

$$\omega_m = \int \frac{1}{J}(T_e - T_m - B\omega_m) \tag{3.14}$$

$$\theta_e = \frac{p}{2}\int \omega_m \tag{3.15}$$

Equations (3.8), (3.12), (3.13), (3.14) and (3.15) were utilized to create a mathematical model of the IPMSM with dynamic behavior in Simulink as illustrated in [Figure 3.3].

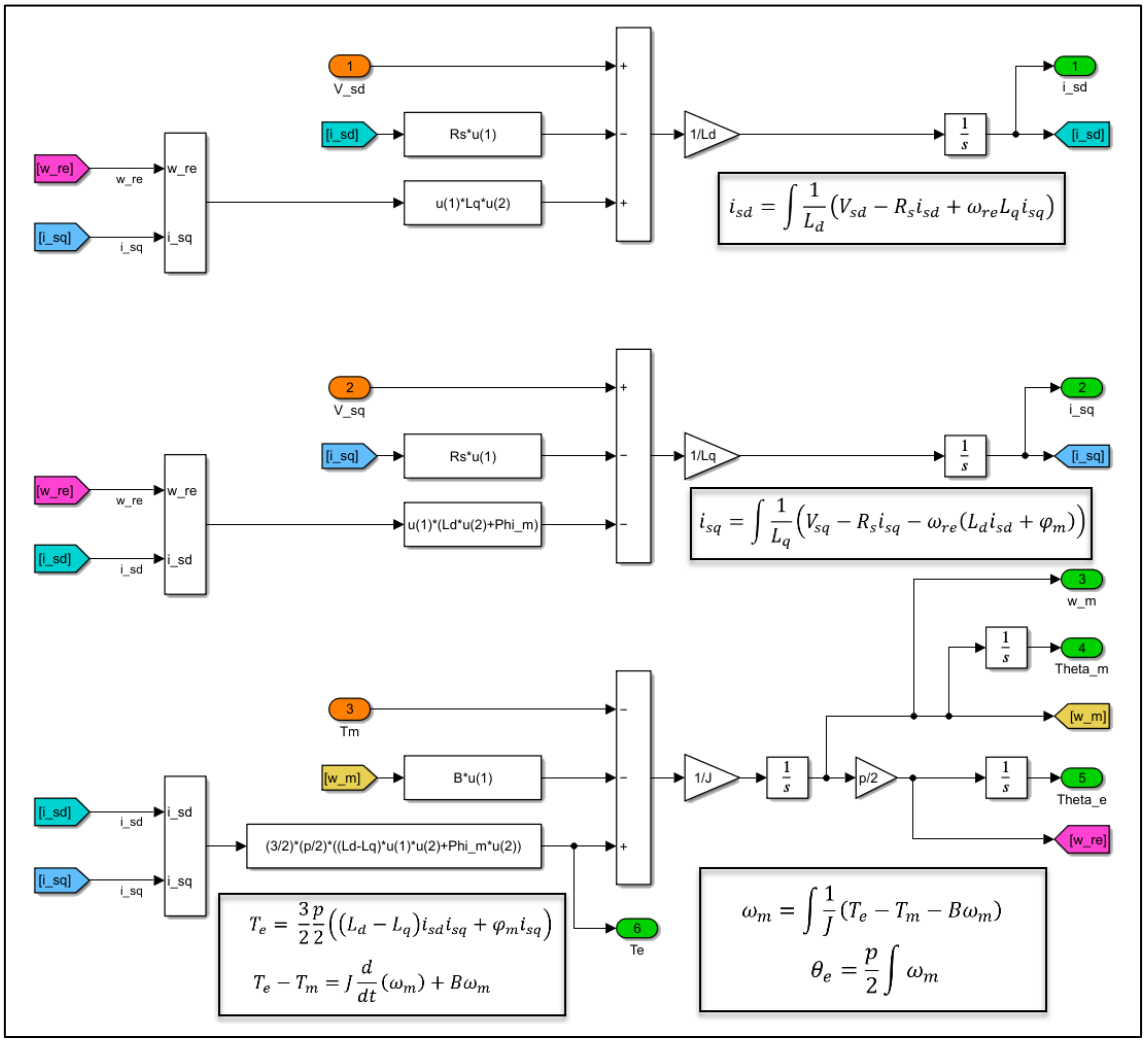

Figure 3.3 IPMSM model created in Simulink

Model inputs are (marked orange) and outputs are (marked green). Inputs (1&2) are the transformed voltage vectors in the $d-q$ reference frame. With input (3), it is possible to introduce load torque to the motor. The outputs (1&2) are stator currents that need to be transformed back to 3-phase system. The process of transformation of the current and voltages are discussed further in the following chapters. Output (3&4) are the mechanical speed and position of the rotor shaft whereas output (5) is the angular position of the stator magnetic field and output (6) is the electromagnetic torque.

3.2 Park Transformation

An introduction to the transformation of vectors is discussed in [Chapter 2.6]. Park transformation was introduced in the early 1920s by Robert H. Park. It converts the sinusoidal waveform of the time varying voltages and currents in a 3-phase system into a synchronously rotating reference frame of 2-axis representation like that of direct current (DC). The two components created as a result are the direct (d) and quadrature (q) axis components as in [Figure 3.4]. This transformation can be applied to any variable under transformation, mainly voltage, current, flux linkage and electric charge.

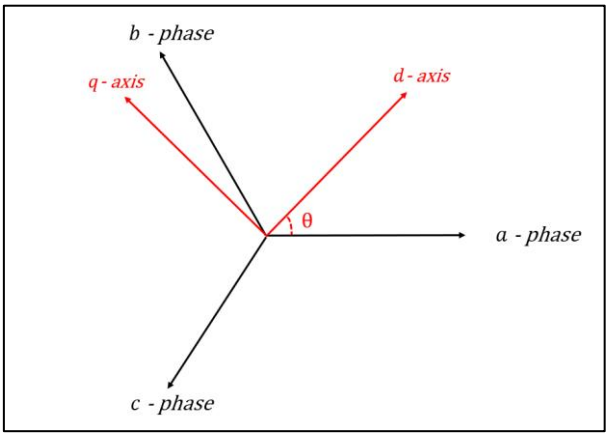

Figure 3.4 Park Transformation

Equations representing both the Park and inverse Park transformation is shown in equation (3.16) and (3.17) as presented in [7]. Where (y) represents the variable under transformation.

$$[y_{dq0}] = T_{dq0}(\theta)[y_{abc}]$$

$$Park\ abc\ to\ dq0 \quad \begin{bmatrix} y_d \\ y_q \\ y_0 \end{bmatrix} = \frac{2}{3}\begin{bmatrix} \cos(\theta) & \cos(\theta - \frac{2\pi}{3}) & \cos(\theta + \frac{2\pi}{3}) \\ -\sin(\theta) & -\sin(\theta - \frac{2\pi}{3}) & -\sin(\theta + \frac{2\pi}{3}) \\ \frac{1}{2} & \frac{1}{2} & \frac{1}{2} \end{bmatrix}\begin{bmatrix} y_a \\ y_b \\ y_c \end{bmatrix} \quad (3.16)$$

$$[y_{abc}] = T_{dq0}^{-1}(\theta)[y_{dq0}]$$

$$Inverse\ Park\ dq0\ to\ abc \quad \begin{bmatrix} y_a \\ y_b \\ y_c \end{bmatrix} = \begin{bmatrix} \cos(\theta) & -\sin(\theta) & 1 \\ \cos(\theta - \frac{2\pi}{3}) & -\sin(\theta - \frac{2\pi}{3}) & 1 \\ \cos(\theta + \frac{2\pi}{3}) & -\sin(\theta + \frac{2\pi}{3}) & 1 \end{bmatrix}\begin{bmatrix} y_d \\ y_q \\ y_0 \end{bmatrix} \quad (3.17)$$

The above-mentioned park transformation is also known as cosine-based park transformation as shown in [Figure 3.5]. This happens when the $(d-axis)$ of the rotating frame is aligned with the a-phase at time $(t=0)$. However, simulating this using a software would result in initial disruption in the angle theta. In the simulation of IPMSM in Simulink, a type of transformation called sine-based Park transformation is preferred. This is when the $(d-axis)$ of the rotating frame is aligned 90° behind the a-phase at time $(t=0)$ as illustrated in [Figure 3.5]. This would result in a modified equation as presented in (3.18) and (3.19) for park and inverse park transformation. Where (y) represents the variable under transformation.

$$[y_{dq0}] = T_{dq0}(\theta)[y_{abc}]$$

$$Park \quad abc\ to\ dq0 \qquad \begin{bmatrix} y_d \\ y_q \\ y_0 \end{bmatrix} = \frac{2}{3}\begin{bmatrix} \sin(\theta) & \sin(\theta-\frac{2\pi}{3}) & \sin(\theta+\frac{2\pi}{3}) \\ cos(\theta) & \cos(\theta-\frac{2\pi}{3}) & \cos(\theta+\frac{2\pi}{3}) \\ \frac{1}{2} & \frac{1}{2} & \frac{1}{2} \end{bmatrix}\begin{bmatrix} y_a \\ y_b \\ y_c \end{bmatrix} \tag{3.18}$$

$$[y_{abc}] = T_{dq0}^{-1}(\theta)[y_{dq0}]$$

$$Inverse\ Park \quad dq0\ to\ abc \qquad \begin{bmatrix} y_a \\ y_b \\ y_c \end{bmatrix} = \begin{bmatrix} \sin(\theta) & cos(\theta) & 1 \\ \sin(\theta-\frac{2\pi}{3}) & \cos(\theta-\frac{2\pi}{3}) & 1 \\ \sin(\theta+\frac{2\pi}{3}) & \cos(\theta+\frac{2\pi}{3}) & 1 \end{bmatrix}\begin{bmatrix} y_d \\ y_q \\ y_0 \end{bmatrix} \tag{3.19}$$

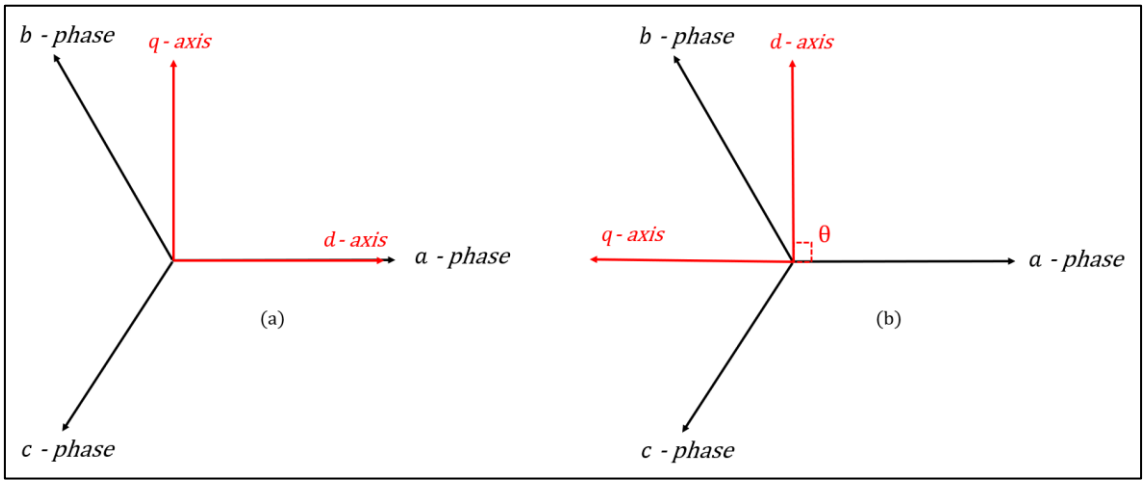

Figure 3.5 Park Transformation (a) Cosine-based at t=0, (b) Sine-based at t=0

The input of the IPMSM model presented in [Figure 3.3] comes from a voltage source inverter (VSI). 3-phase input voltage needs to be converted into 2-phase rotating (d, q) frame to simplify the control of the motor. Likewise, the output current along the (d, q) frame must be transferred back to 3-phase current for the implementation of DTC logic using equations (3.18) and (3.19) as illustrated in [Figure 3.6]. It is important to note that, $d - q$ transformation is not part of the DTC logic. It is introduced in the simulation to have a complete model of the IPMSM as shown in [Figure 3.7].

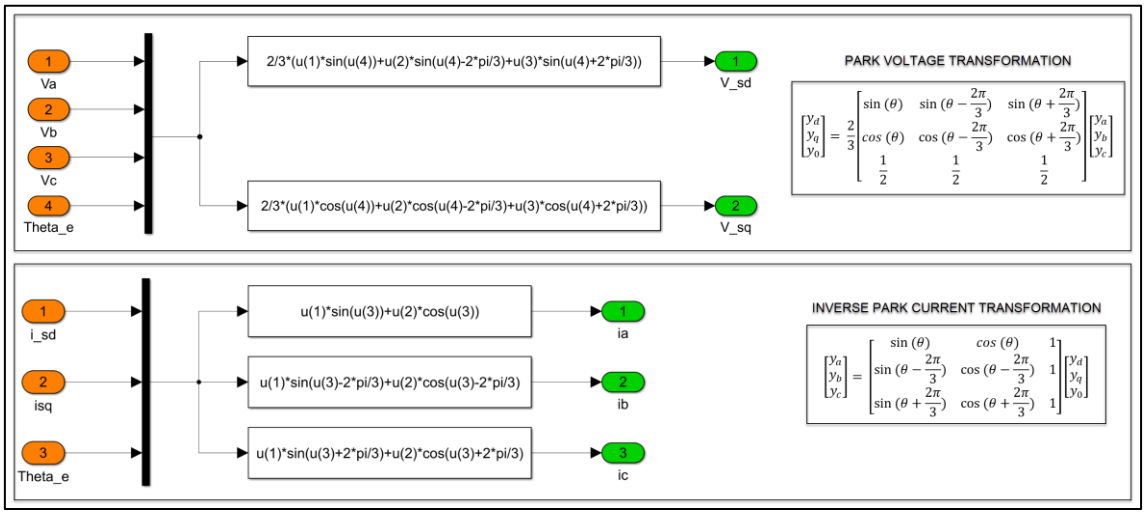

Figure 3.6 Park and Inverse Park transformation on voltage and current

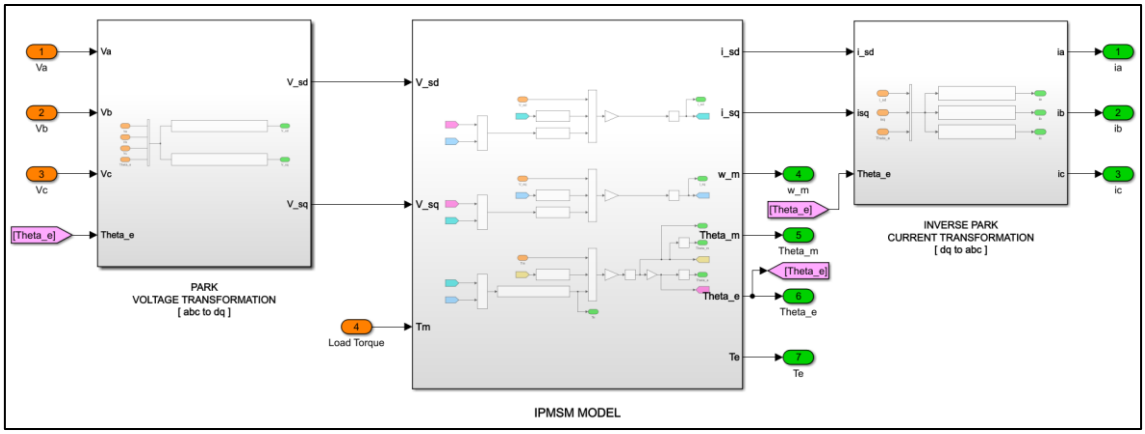

Figure 3.7 Complete IPMSM model with voltage and current transformations

3.3 Voltage Source Inverter

A 2-level, 3-phase Voltage Source Inverters (VSI) are used in PMSM drive systems to provide the 3-phase voltages (V_a, V_b, V_c) (marked orange) in the [Figure 3.7]. This is achieved by using two switches per phase, resulting in a total of six switches for a 3-phase inverter. The term "2-level" comes from the fact that output waveform generated for each phase has the possibility to switch between two voltage level of the DC bus, one positive and one negative. Inverters and their switching states are discussed in this chapter.

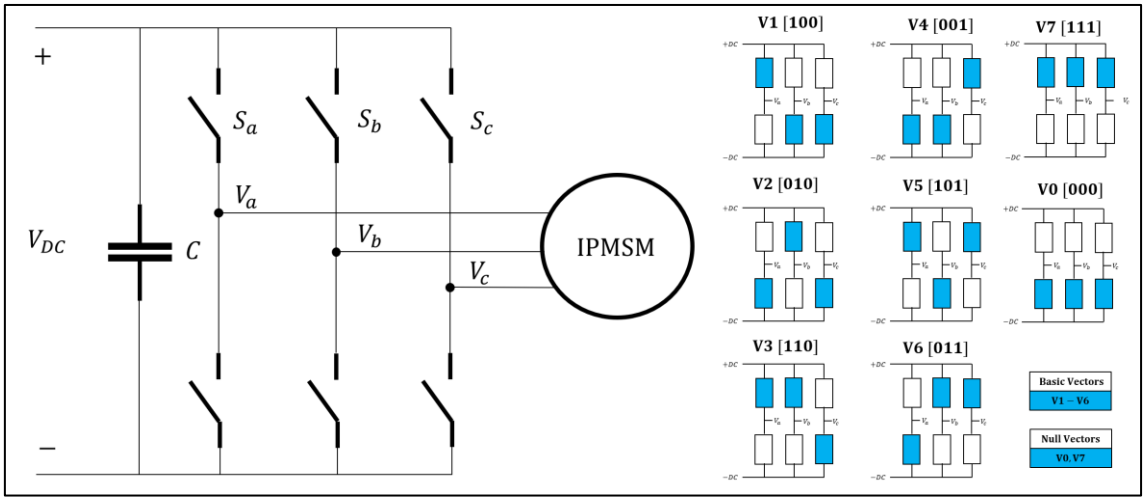

Figure 3.8 2-level 3-phase voltage source inverter

In an inverter (S_a, S_b, S_c) there are two switches per phase. These switches are typically implemented using the two Insulated Gate Bipolar Transistors (IGBT's) per phase. A circuit diagram of a 2-level inverter and switching combinations are presented in [Figure 3.8]. The states of these switches determine the output voltages to the motor. It is important to note that, at any one-time instance, only one of the two switches along a phase is closed. This leads to a total of eight possible switching combinations$(V_0\ to\ V_7)$. The control circuits that generate these switching patterns ensure proper synchronization to prevent overlapping of the switching states. Switch activating signals called gate pulses, their generation, and selection of voltage vectors along with the sector selection principles, are discussed further in the following chapters. Switching between two voltage levels at a high frequency gives an average output voltage using the method of PWM as shown in equation (3.20), which then is used to create a model of the VSI in Simulink as shown in [Figure 3.9].

$$V_a = \frac{1}{3}V_{DC}(2S_a - S_b - S_c)$$
$$V_b = \frac{1}{3}V_{DC}(2S_b - S_a - S_c) \qquad (3.20)$$
$$V_c = \frac{1}{3}V_{DC}(2S_c - S_a - S_b)$$

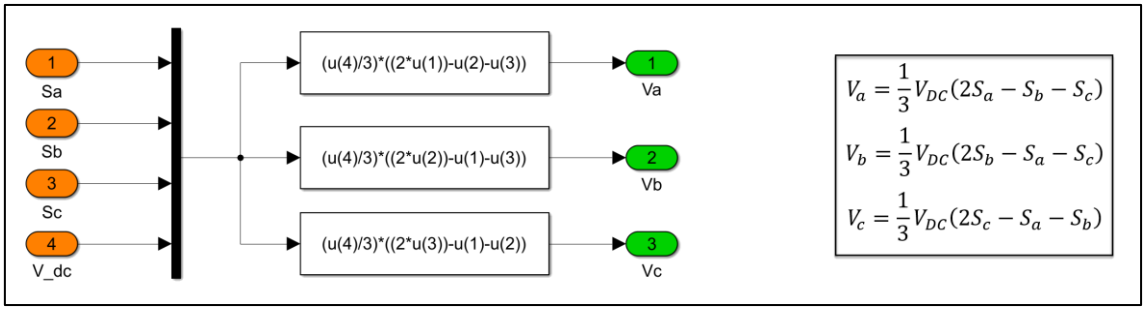

Figure 3.9 Model of Voltage Source Inverter

3.4 DTC on IPMSM

The fundamental concept behind DTC, is crucial for gaining a profound insight into the generation of gate pulses that activates the switches (S_a, S_b, S_c) presented in [Figure 3.9]. [Chapter 2.2] briefly discusses how the DTC achieves direct control of the electromagnetic torque and flux using separate hysteresis controllers that subsequently chooses the appropriate voltage vectors from a switching table.

In [Figure 3.9], there are two control loops. The inner loop has the torque and flux hysteresis controller, Clarke transformation, sector selection table and an estimator that calculates actual torque and flux generated by the motor. It is important to note that only Clarke transformation is used while implementing DTC control. The outer loop uses an encoder to measure the rotor speed and initial rotor position. Even though DTC can be a 'sensorless' type control, the implementation of sensor less control is not focused on this thesis. The stator flux (φ_s) and the electromagnetic torque (T_e) of an IPMSM can be estimated using the stationary reference frame $(\alpha - \beta)$ as in [7].

$$\varphi_{s\alpha} = \int (V_{s\alpha} - R_s i_{s\alpha})\, dt \tag{3.21}$$

$$\varphi_{s\beta} = \int (V_{s\beta} - R_s i_{s\beta})\, dt \tag{3.22}$$

$$\varphi_s = \sqrt{\varphi_{s\alpha}^2 + \varphi_{s\beta}^2} \tag{3.23}$$

$$\theta_s = arctan\left(\frac{\varphi_{s\beta}}{\varphi_{s\alpha}}\right) \tag{3.24}$$

$$T_e = \frac{3}{2}\frac{p}{2}(\varphi_{s\alpha} i_{s\beta} - \varphi_{s\beta} i_{s\alpha}) \tag{3.25}$$

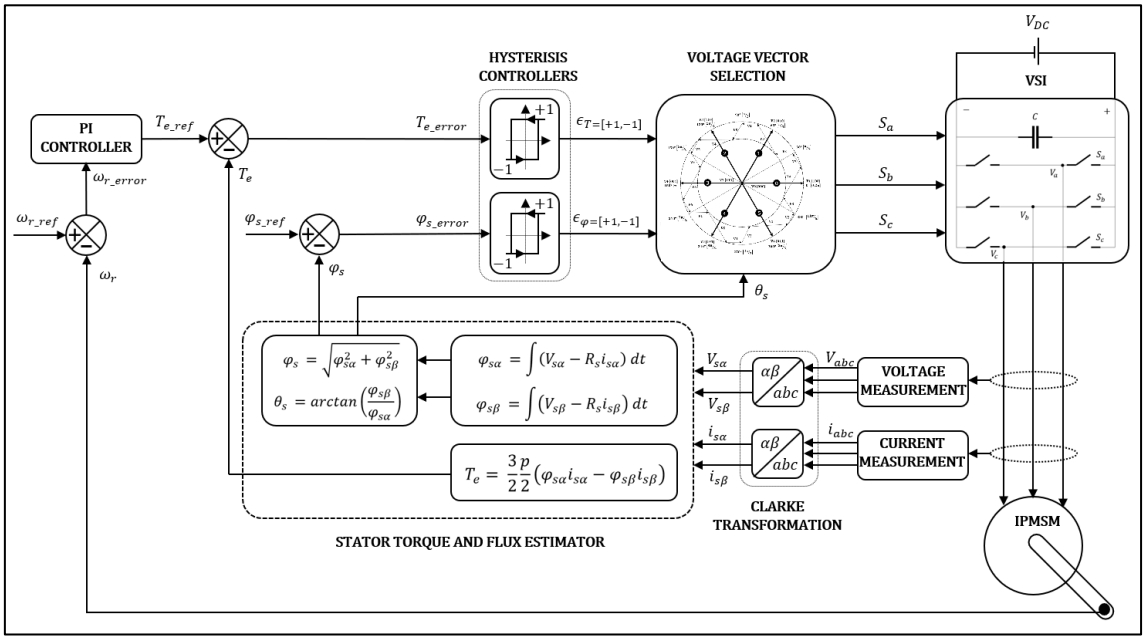

Figure 3.10 Principle of DTC strategy

Where:

$V_{s\alpha}, V_{s\beta}$	Stator voltages in the $\alpha - \beta$ reference frame
$i_{s\alpha}, i_{s\beta}$	Stator currents in the $\alpha - \beta$reference frame
$\varphi_{s\alpha}, \varphi_{s\beta}$	Stator flux linkage in the $\alpha - \beta$ reference frame
R_s	Stator resistance
p	Number of poles of the rotor

The estimated values of the torque and flux are then compared to the reference values provided which generates an error signal. The generated error is then quantified within the hysteresis band limits of flux and torque controller. Using the equations (3.21), (3.22), (3.23), (3.24) and (3.25), a simulation model of the flux and torque estimation is created in Simulink as shown in [Figure 3.11].

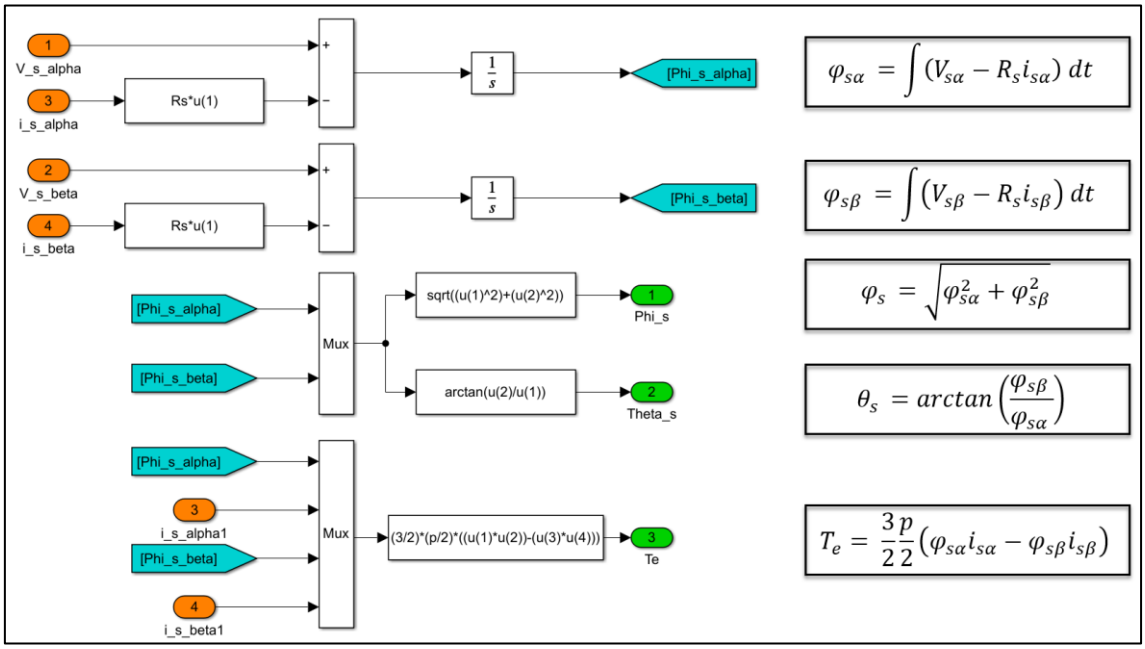

Figure 3.11 Model of torque and flux estimator

3.5 Clarke Transformation

Clarke transformation was first introduced by Edith Clarke and is used for transforming 3-phase variables and circuits into a stationary reference frame. During Clarke transformation the 3-phase variable (a, b, c) (voltage, current, flux linkage or electric charge) is converted into fixed 2-phase stationary frame (α, β).

The four inputs (marked orange) in [Figure 3.10], $(V_{s\alpha}, V_{s\beta}, i_{s\alpha}, i_{s\beta})$ have to be transformed from the measured voltage (V_a, V_b, V_c) and the measured current (i_a, i_b, i_c) in the circuit. Transformation along with simulation model creation is discussed in this chapter.

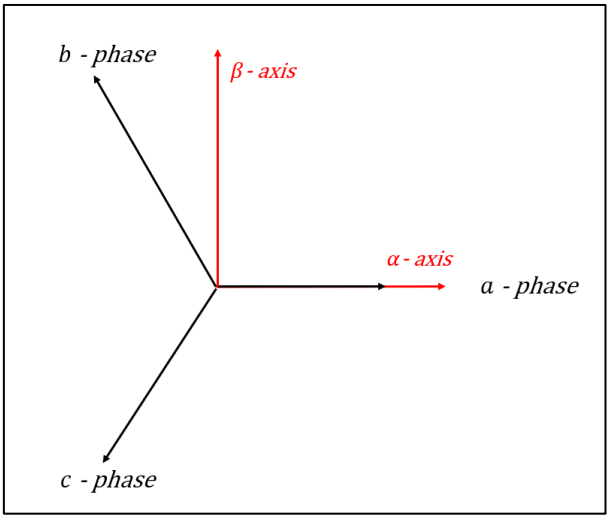

Figure 3.12 Clarke Transformation

Transformation uses ($a - phase$) as a reference with a variable (x) in [Figure 3.12].

$$x_\alpha = x_a \tag{3.26}$$

$$x_\beta = \frac{2x_b + x_a}{\sqrt{3}} \tag{3.27}$$

To enable the conversion back to 3-phase frames, a zero component is added into the operation. Where (x) represents the variable under transformation. Clarke transformation of the variable as well as the inverse Clarke transformation is shown in equation (3.28) and (3.29) as presented in [7].

$$[x_{\alpha\beta0}] = T_{\alpha\beta0}[x_{abc}]$$

$$Clarke \quad abc\ to\ \alpha\beta0 \qquad \begin{bmatrix} x_\alpha \\ x_\beta \\ x_0 \end{bmatrix} = \frac{2}{3}\begin{bmatrix} 1 & -\frac{1}{2} & -\frac{1}{2} \\ 0 & \frac{\sqrt{3}}{2} & -\frac{\sqrt{3}}{2} \\ \frac{1}{2} & \frac{1}{2} & \frac{1}{2} \end{bmatrix}\begin{bmatrix} x_a \\ x_b \\ x_c \end{bmatrix} \tag{3.28}$$

$$[x_{abc}] = T^{-1}_{\alpha\beta0}[x_{\alpha\beta0}]$$

$$Inverse\ Clarke \quad \alpha\beta0\ to\ abc \qquad \begin{bmatrix} x_a \\ x_b \\ x_c \end{bmatrix} = \begin{bmatrix} 1 & 0 & 1 \\ -\frac{1}{2} & \frac{\sqrt{3}}{2} & 1 \\ -\frac{1}{2} & -\frac{\sqrt{3}}{2} & 1 \end{bmatrix}\begin{bmatrix} x_\alpha \\ x_\beta \\ x_0 \end{bmatrix} \tag{3.29}$$

The simulation model presented in [Figure 3.13] only uses the Clarke transformation. The inverse Clarke transformation deals with transforming back to (a, b, c) frame. However, in DTC, there is no need to perform this transformation because the voltage vectors are directly selected by the switching table and sector selection.

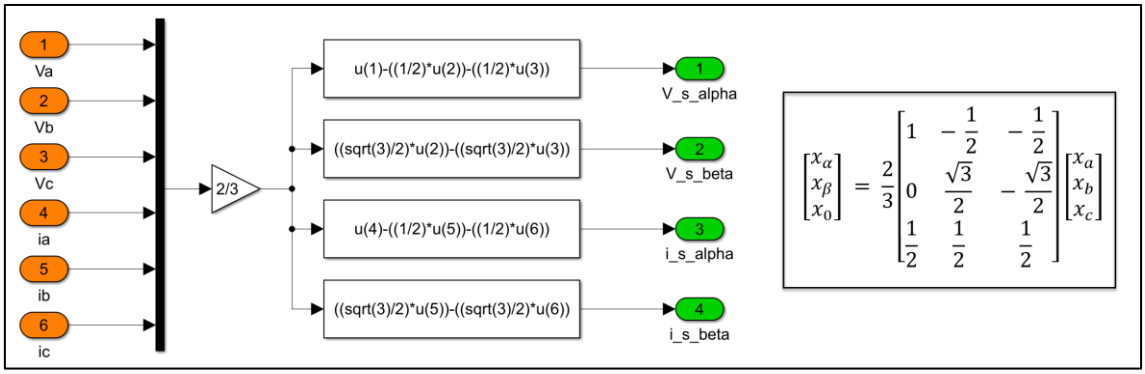

Figure 3.13 Model of Clarke transformation

3.6 Sector Selection and switching tables.

The input signals (S_a, S_b, S_c) presented in [Figure 3.9] that determine the output voltage of the inverter is selected from a switching table based on the estimated torque and flux values calculated and presented in [Figure 3.10]. The switching table and the sector selection for a typical DTC drive is covered in this chapter. To properly select a voltage vector, it is important to estimate the initial value of the Stator flux vector magnitude (φ_s) and its angle (θ_s) at time $(t = 0)$. The number of voltage vectors available for selection depends on the voltage level of the inverter. A 2-level inverter can generate six fundamental voltage vectors $(V_1\ to\ V_6)$ and two null vectors$(V_0$ and $V_7)$ with zero magnitude in the (α, β) system. To simplify the identification of the stator flux vector phases, the (α, β) system is divided into six sectors $(0\ to\ 5)$, each 60° apart. These sectors also help to keep the stator flux trajectory almost smoothly circular. Each sector lies within an angle range of $(-30°\ to\ 30°)$. Assuming, the stator flux vector(φ_s) to be in sector (0) at time $(t = 0)$, the effects of applying four non-zero fundamental vectors $(V_2, V_3, V_5\ \&\ V_6)$ for one switching period considering a counterclockwise rotation is presented in [Figure 3.14].

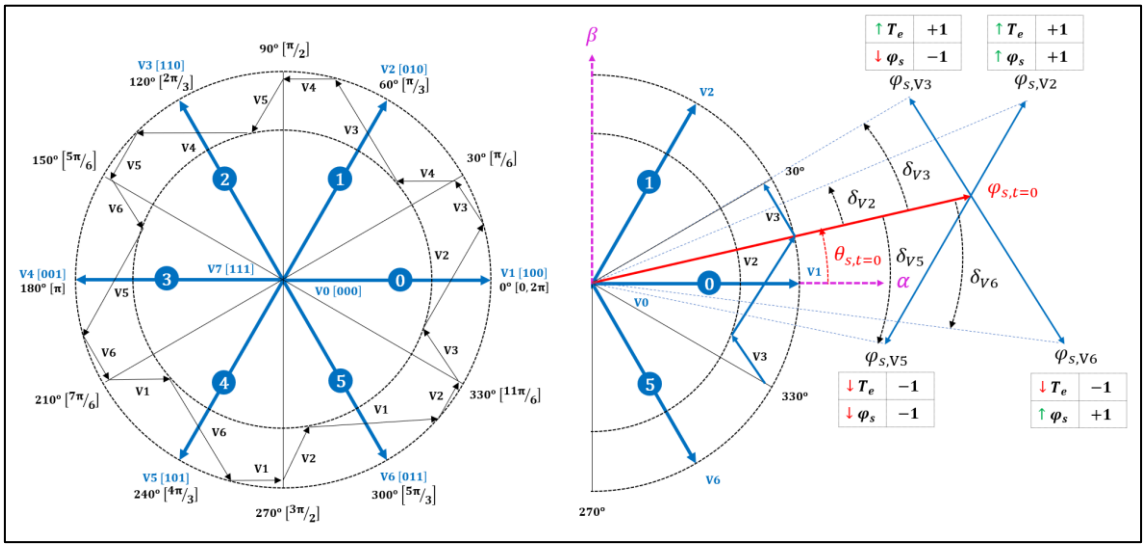

Figure 3.14 Sector and switching table selection

In [Figure 3.14] it is evident that the stator flux vector (φ_s) rotates in counterclockwise direction when the non-zero voltage vectors $(V_2\ or\ V_3)$ are applied. This creates a positive change of the load/torque angle (δ). Meaning that if the torque needs to be increased, when the stator flux is in sector 1, then the inverter must use the switching combination $(V_2\ or\ V_3)$. In that case, the decision to choose either vector $(V_2\ or\ V_3)$ depends on the stator flux demand. Vector (V_2) provides an increase in magnitude of the stator flux whereas (V_3) decreases the magnitude of the stator flux as shown prior. In sector (0), it is important to note that, the voltage vectors $(V_0, V_1, V_7\ \&\ V_4)$ are not used since they do not produce enough load angle variation when compared to $(V_2, V_3, V_5\ \&\ V_6)$. For other sectors, there similarly exist four active voltage space vectors that can be selected based on the torque and flux demand. This demonstrates that the stator flux linkage is circular. However, the width of the circle is decided by the bandwidth of the hysteresis controllers shown in [Figure 3.15].

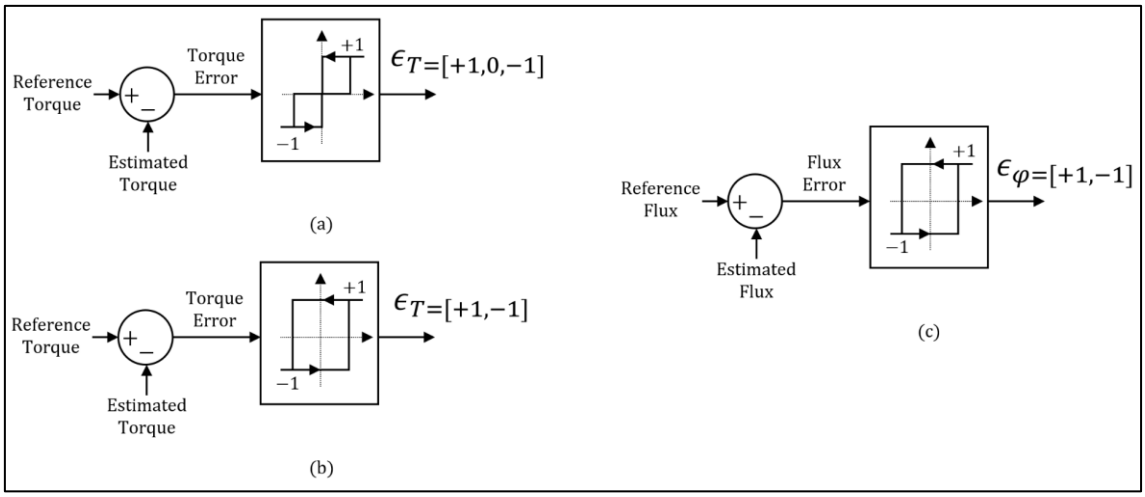

Figure 3.15 Hysteresis (a) Torque of IM (b) Torque of IPMSM (c) Flux control

A 2-level hysteresis controller can be used in the flux control of DTC for all motor types. However, torque hysteresis controller used in DTC of IM drive has three output levels $(+1, 0, -1)$ where $+1$ and -1 indicates that an increase and decrease in torque is required. (0) state indicates that the calculated torque is within the band limits of the hysteresis controller which also indicates that a sudden change of torque is not required. During a (0) state, a zero vector is applied to the IM, which makes sure that the stator flux stays in its initial position. This concept is applicable to IM since the stator flux linkage is exclusively determined by the stator voltage. However, when a zero vector is applied to an IPMSM, the stator flux will not stay in the initial position due to the presence of permanent magnet flux in the rotor. Consequently, the hysteresis controller of an IPMSM does not use (0) state for the torque control. Instead, a 2-level hysteresis controller is used [9]. Therefore, the zero vectors $(V_0\ \&\ V_7)$ are commonly used in the DTC control of IM drives and not in IPMSM drives. The switching table for IPMSM used in this study shown in [Table 3.1] has zero vectors 'greyed out' to highlight this.

Table 3.1 Switching table for DTC control of IPMSM

Stator Flux Error	Electromagnetic Torque Error	Sector Selection (θ)					
		θ [0] $[\pi/6 \& 11\pi/6]$	θ [1] $[\pi/2 \& \pi/6]$	θ [2] $[5\pi/6 \& \pi/2]$	θ [3] $[7\pi/6 \& 5\pi/6]$	θ [4] $[3\pi/2 \& 7\pi/6]$	θ [5] $[11\pi/6 \& 3\pi/2]$
-1 [0]	-1 [0]	V4	V5	V1	V3	V2	V6
	0 [1]	V0	V7	V0	V7	V0	V7
	1 [2]	V2	V6	V4	V5	V1	V3
1 [1]	-1 [0]	V5	V1	V3	V2	V6	V4
	0 [1]	V7	V0	V7	V0	V7	V0
	1 [2]	V3	V2	V6	V4	V5	V1

To reiterate, there are three outputs from the torque and flux estimator model presented in [Figure 3.10]: torque, flux & angle (θ). The calculated electromagnetic torque and the stator flux is compared with a reference torque and flux to generate an error signal that is controlled within the bands of a torque and flux hysteresis controllers as shown in [Figure 3.15, b, c]. The torque and the flux error along with the (theta) passed through a modulo operation is used as the input to the switching table script to generate the logic presented in [Table 3.1]. A 3D look-up table was used to implement this logic in Simulink as shown in [Figure 3.16].

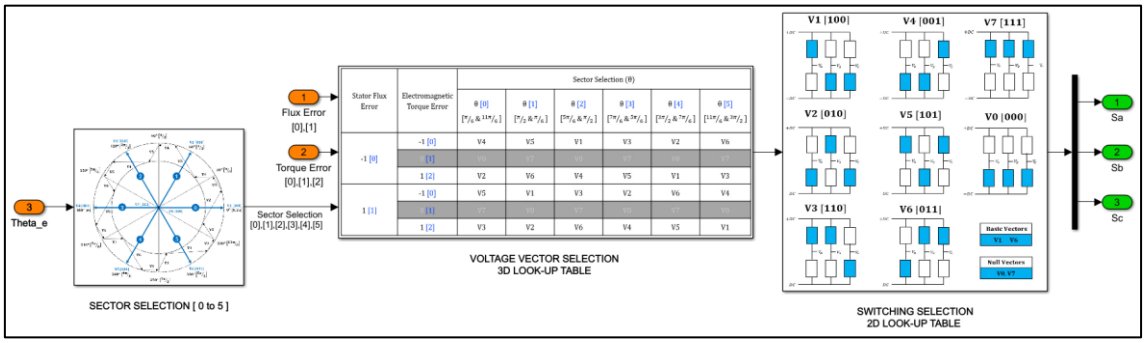

Figure 3.16 Sector selection and voltage vectors using switching tables

3.7 Implementation

The principles and theories outlined in the previous sections have been utilized to construct a comprehensive model of an Interior Permanent Magnet Synchronous Motor (IPMSM), which is regulated via Direct Torque Control (DTC). The model developed in Simulink is presented in [Figure 3.17]. There are a few modifications which were made to the model to obtain a better result. Given that the model incorporates an Interior Permanent Magnet Synchronous Motor (IPMSM), it calculates the electromagnetic torque by considering the impacts of the permanent magnet flux as well as the d-axis and q-axis inductances. The torque hysteresis controller is fed with this torque as feedback. Similarly, the theta obtained from the same model is used for the sector selection. This is further

discussed in the validation phase. The parameters for the model was obtained from a research paper published on this subject [10].

Number of Phases	: 3
Voltage (DC)	: 300 V
Stator Phase Resistance [Rs]	: 4.7 Ω
Inductances [Ld, Lq]	: 0.0133 H, 0.0133 H
Permanent Magnet Flux [Phi_m]	: 0.264 W_b
Inertia [J]	: 0.00062 $Kg.m^2$
Viscous Damping [B]	: 0.0003035 Nms
Number of Poles [p]	: 8
Rated Speed	: 3000 rpm
Rated Torque	: 2.1 Nm

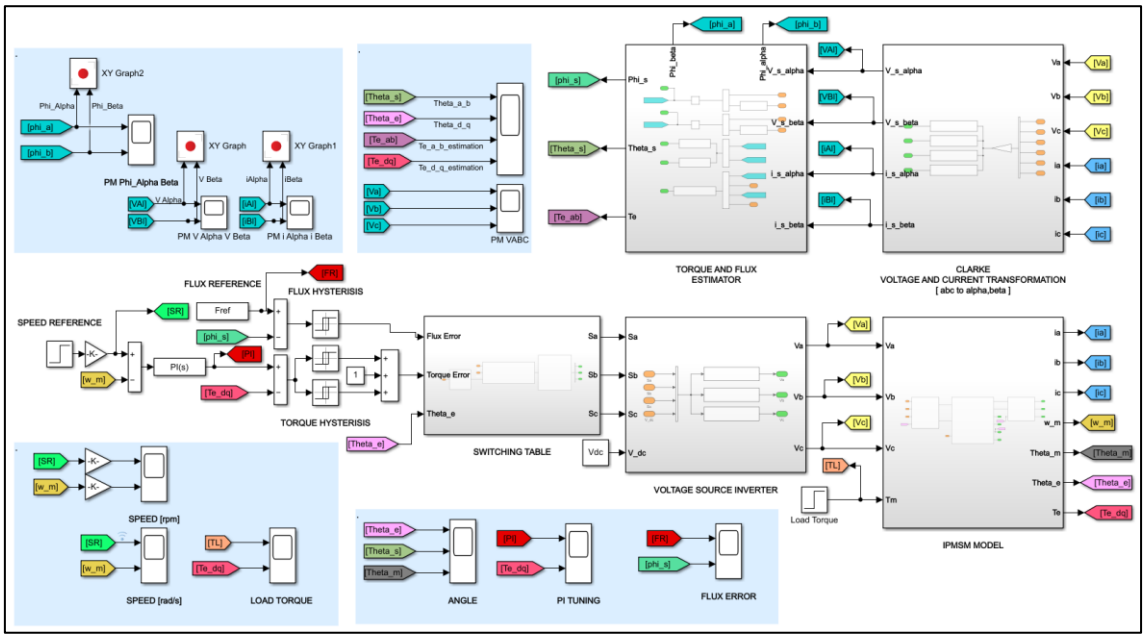

Figure 3.17 DTC control of IPMSM

Originally, the scope of the project included a practical validation of the simulation model with an actual IPMSM used for an electric vehicle. However, it became impractical to complete this stage of the project within the planned timeframe. As a result, the approach was pivoted towards an alternative method of validation. The validation of the simulation was carried out against a peer-reviewed article in the same discipline. A speed reference of 80% of the rated speed was input to the PI controller, and a load torque equivalent to 95% of the rated torque was fed into the IPMSM model. The tuning of the controller was optimized to minimize controller overshoots and settling time. The model could be further refined by substituting simulated voltages and currents with real-life equivalents.

4 Validation

4.1 IPMSM Validation

To prevent complication during the development process of the simulation model and to simplify problem-solving, each sub system in the DTC control is separately validated and confirmed to be accurate prior to the creation of the final model. The developed IPMSM model illustrated in [Figure 3.6] was validated against a pre-built model in Simulink.

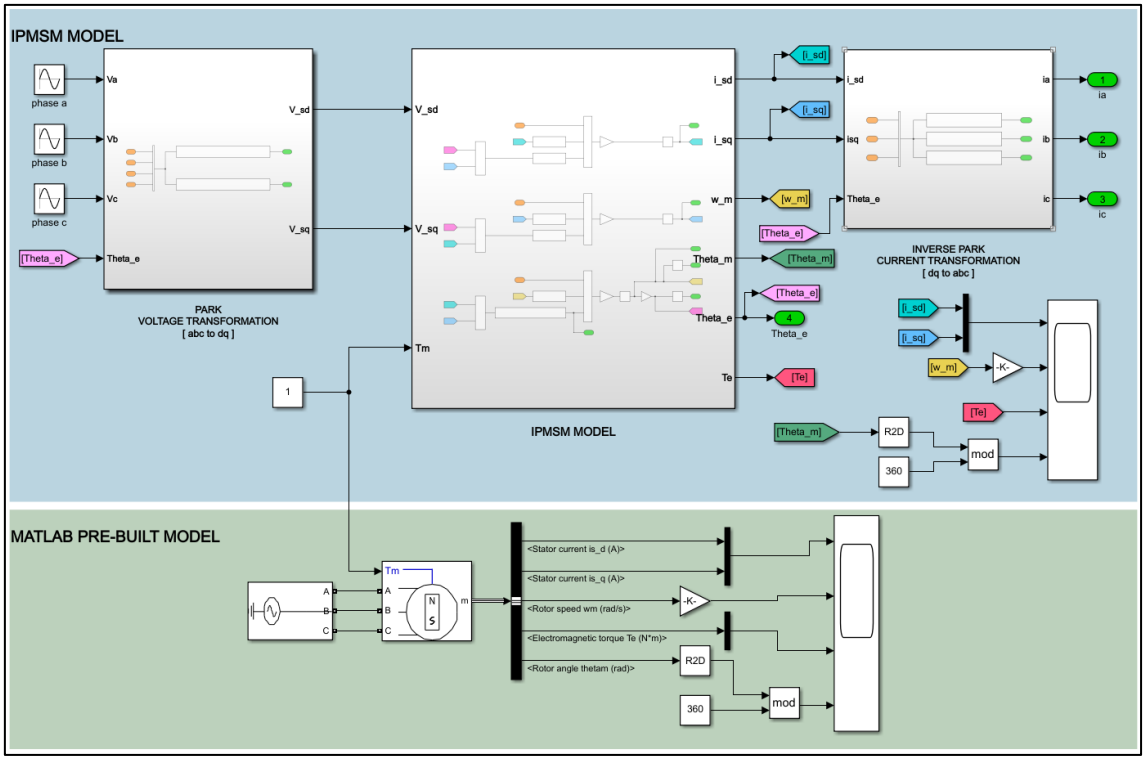

Figure 4.1 IPMSM validation against Matlab pre-built model

The [Figure 4.1] shows a 3-phase voltage (V_a, V_b, V_c), transformed using sine-based park transformation and fed to the IPMSM model as $(V_{sd}$ & $V_{sq})$. The three outputs that are used in the DTC control are the mechanical speed of the rotor shaft (ω_m) which is used as the feedback signal to the PI controller, the electromagnetic torque (T_e) which used as the estimated torque to calculate the error for the torque hysteresis controllers and the estimated angular position of the stator flux (θ_e) which is used to sector selection within the algorithm. It is important to note that the plotted signal for validation in [Figure 4.2] is the mechanical rotor position of (θ_m) and this is used only for a comparison with the pre-built model in Matlab. The result of the validation presented in [Figure 4.2] shows that the transformed currents $(i_{sd}$ & $i_{sq})$ along with the other presented results are exactly like the pre-built model. The rotor position has the (θ_m) passed through a modulo operation to have the angle limited between $(0°$ & $360°)$. This plays an important role in the DTC algorithm since the switching table is divided into six sectors and the voltage vectors must be constrained within these six sectors for optimum motor control.

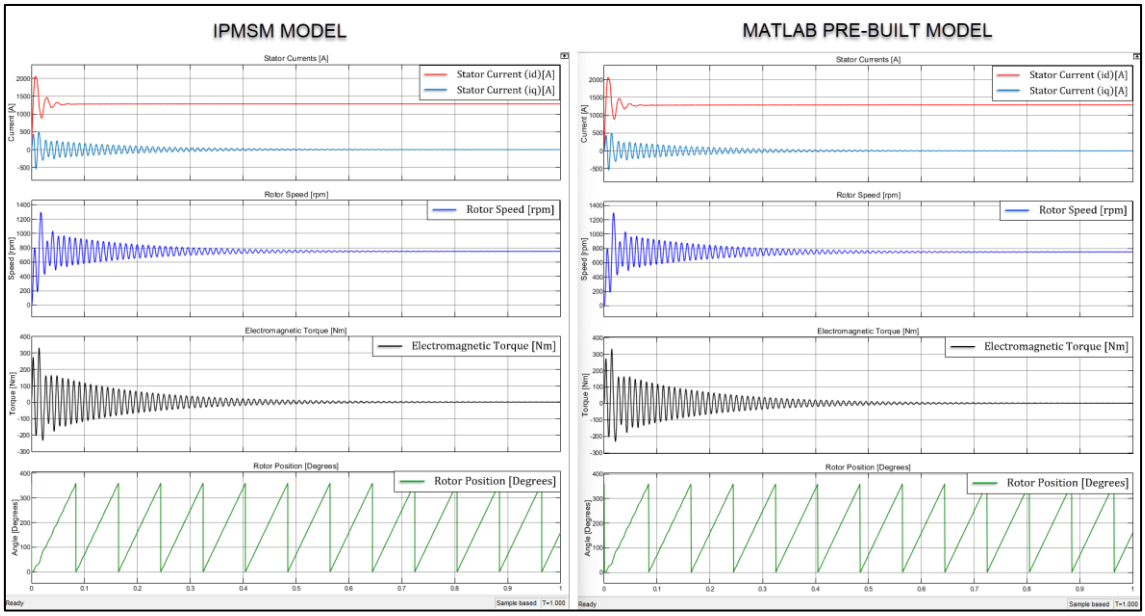

Figure 4.2 Result comparison between developed and pre-built model.

4.2 Sector and switching Table validation.

Typically, sinusoidal PWM method is used to control the amount of voltage that is sent to the motor from an inverter. This involves a carrying wave, modulating wave and a PWM wave, as presented in [Figure 4.3].

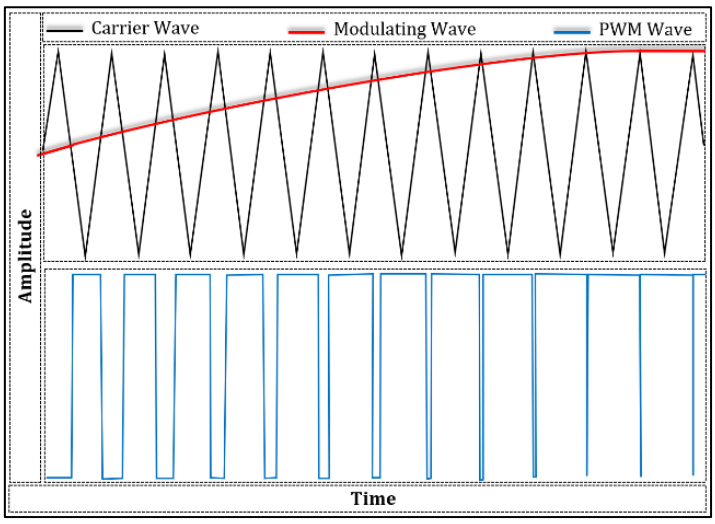

Figure 4.3 Sinusoidal PWM

However, in space vector PWM used in DTC control, there are no carrier waves in the form of triangular waves. Even though the angle theta in [Figure 4.2] looks like a carrier wave, it is simply a modulo operation carried out on the angle theta to help with sector selection. It is important to note that it does not directly influence the shape or timing of the output voltage waveform. Hence referring to theta as a carrier wave in SVPWM would be incorrect.

The selection of accurate voltage vectors from the switching table is the key to a successful DTC implementation. It was noticed that even with a slight change in switching table selection, the model will not work as intended. To avoid this, the switching table was implemented as a look-up table instead of a script for understanding the concept better as well as to make the troubleshooting simpler. Identifying the sector in which the voltage vectors are placed, the modulo operation on the angle theta for selecting a sector, choosing the correct voltage vector from the switching table and finally the selection of the switching states for the inverter switches along with its validation is discussed in this chapter.

Sector selection presented prior in [Figure 3.16] has three steps. A simplified illustration of the steps in converting to tabular format instead of a script is presented in [Figure 4.4]. To validate the precision of the model, sample data was fed into the three inputs of the lookup table. For the first scenario, wherein $(\varphi = 0)$, $(\tau = 1)$, $(\theta = 3)$, the values are chosen from the (brown row) in the second step. The column to be chosen equals the row value of torque, so in the first scenario, the voltage vector selected is V4 [0 0 1]. In a similar manner, for the second scenario where $(\varphi = 0)$, $(\tau = 0)$, $(\theta = 3)$, the (blue row) is the source of values while in the second step. Thus, for this second scenario, the selected voltage vector is V3 [1 1 0].

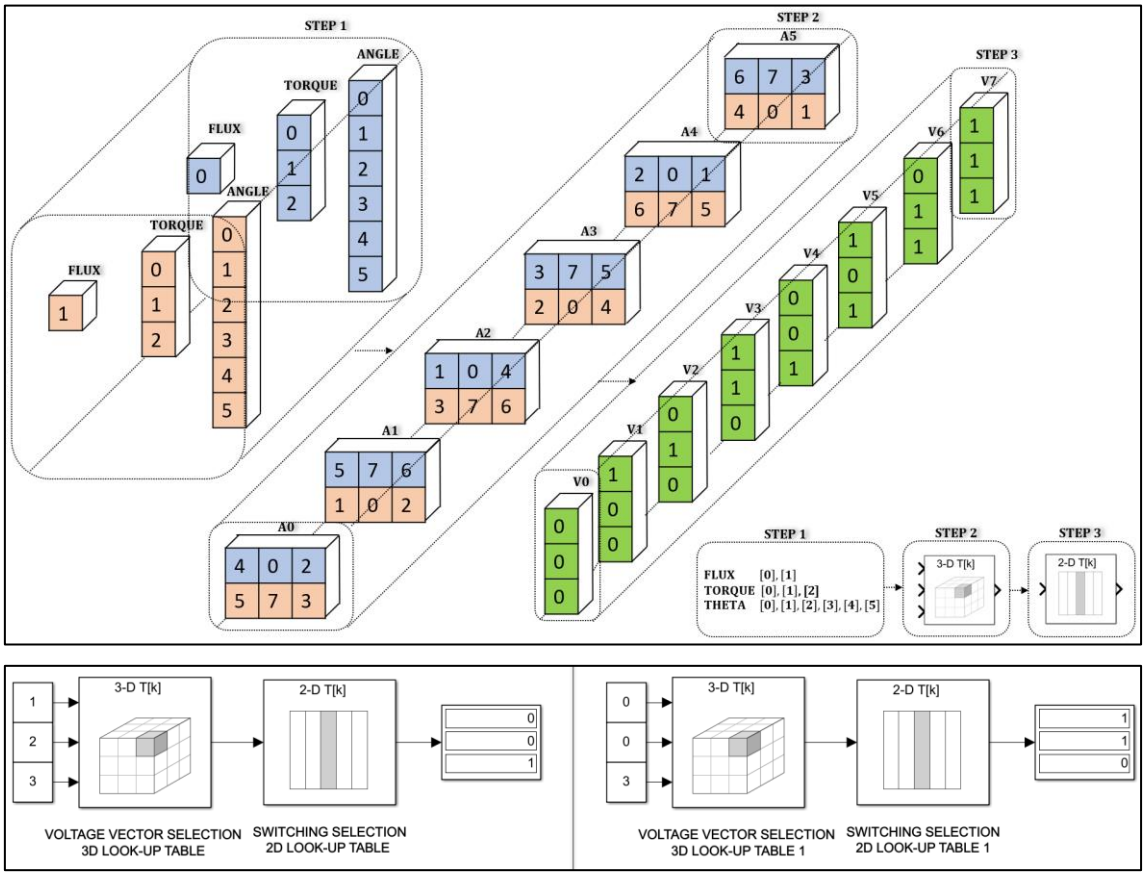

Figure 4.4 Switching state validation

5 Results / Findings

5.1 X-Y Plot of the Voltage Vectors

The result presented in [Figure 5.1] shows the switching pattern of the 3-phase inverter. From [Figure 3.14], it is evident that the selection of voltage vectors from the switching table has a hexagonal pattern. The hexagonal shape is the characteristic representation of inverter output in the (α, β) stationary reference frame. As discussed in the earlier chapters, there are eight possible switching states (six active and two zero states). When these states are represented in the (α, β) reference frame, the six active states form the vertices of a hexagon, and two zero states form the center of the hexagon. Each vertex represents a voltage vector that can be applied to the motor by the inverter.

In DTC, the torque and flux hysteresis controller choose the voltage vectors that maintains the stator flux and torque within the hysteresis bands. Hence the hexagonal shape of the plot signifies that the inverters is operating as intended to produce all the active desired voltage vectors. However, the actual trajectory that the voltage vector follows depends on the operating condition and the response of the controller.

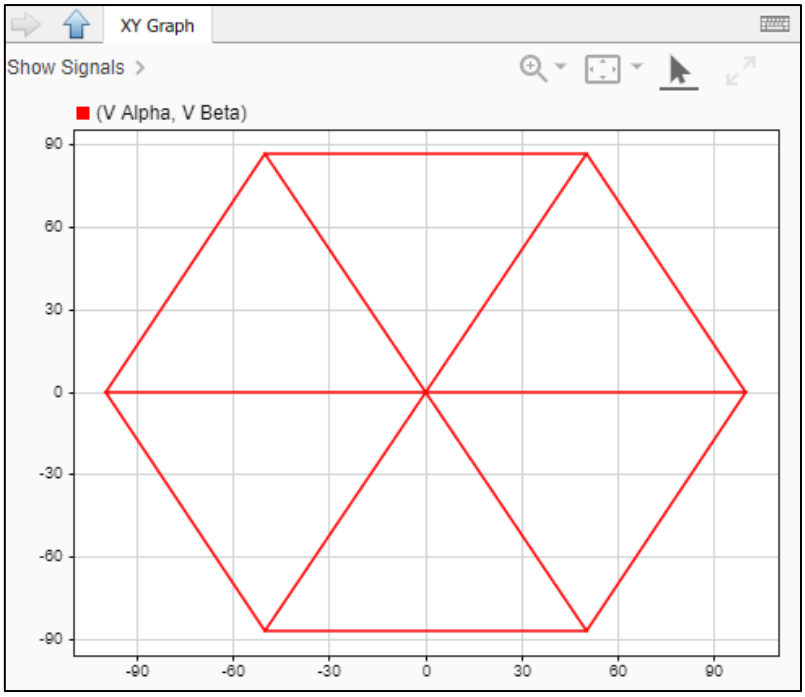

Figure 5.1 X-Y plot - V_α *and* V_β

5.2 X-Y Plot of the Flux Vectors

The result presented in [Figure 5.2] shows the change in the magnitude and length of the stator flux vector based on the motor load and command signals. In this case, the requested speed and load torque are utilized. Each of the hexagonal loops represent a complete electrical cycle of the motor's operation. It is evident that like voltage vectors, the

flux vector pattern is a hexagon and not a circle. This switching action, based on the hysteresis control, can cause the actual flux to trace a path around the reference flux that forms a hexagonal shape when plotted in the X-Y plane. This hexagon is formed due to the specific voltage vectors produced by the six active states of the VSI, which correspond to the six corners of the hexagon.

Hexagonal loop suggests that the motors inductances are not equal in the (d, q) reference frame. This is typical for a IPMSM due to the presence of permanent magnets in the rotor. The multiple concentric hexagonal loops also suggests that the magnitude of the vector changes over time. In DTC, the controller adjusts the stator flux magnitude to control the motor torque. The stator flux should always be within the hysteresis band if the controller is operating as intended. This would mean that there would be a band of concentric hexagonal loops as presented in the plot. The number and spacing between the loops depend on the width of the hysteresis band and the controller performance.

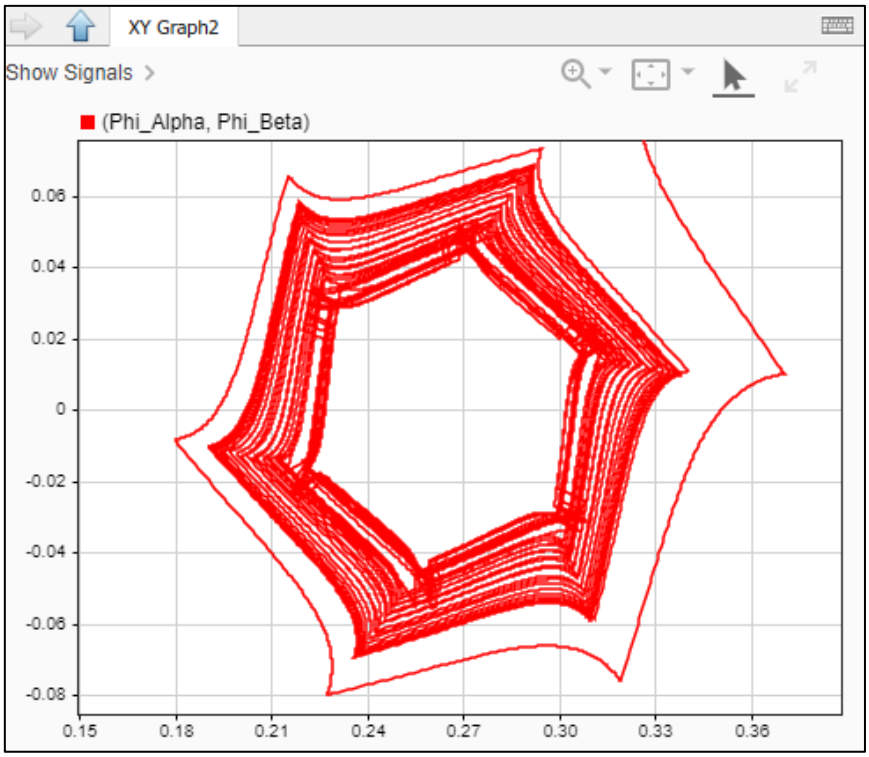

Figure 5.2 X-Y plot - φ_α *and* φ_β

5.3 X-Y Plot and Amplitude of Currents

The results presented in [Figure 5.3] show the transformed currents in the (α, β) reference frame represented in spatial domain. This transformation uses the sine based inverse Park transformation as presented in equation (3.19). When you plot the (i_α) on the $(x - axis)$ and (i_β) on the $(y - axis)$ you get a parametric plot where a function is plotted against another function that uses the same independent variable. In this case, the time. The radius of the circle gives the magnitude of the current vector, and the angle gives the phase.

Since the torque is proportional to the magnitude of current, the circular shape shows that the motor is operating at constant torque level.

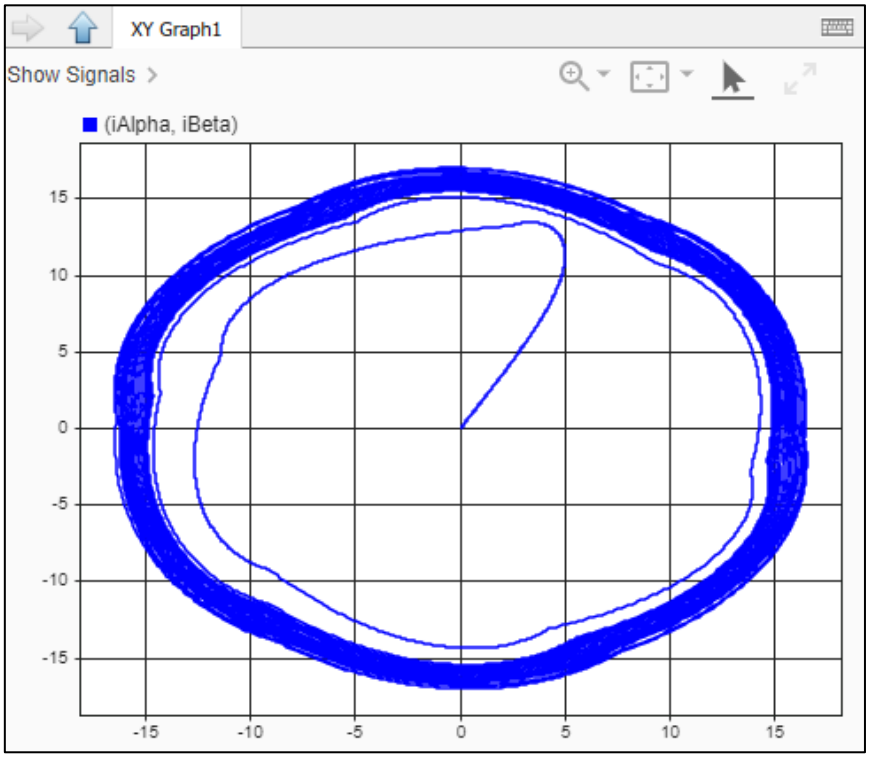

Figure 5.3 X-Y plot - i_α *and* i_β

The results presented in [Figure 5.4] show the transformed currents in the (α, β) reference frame represented in time domain.

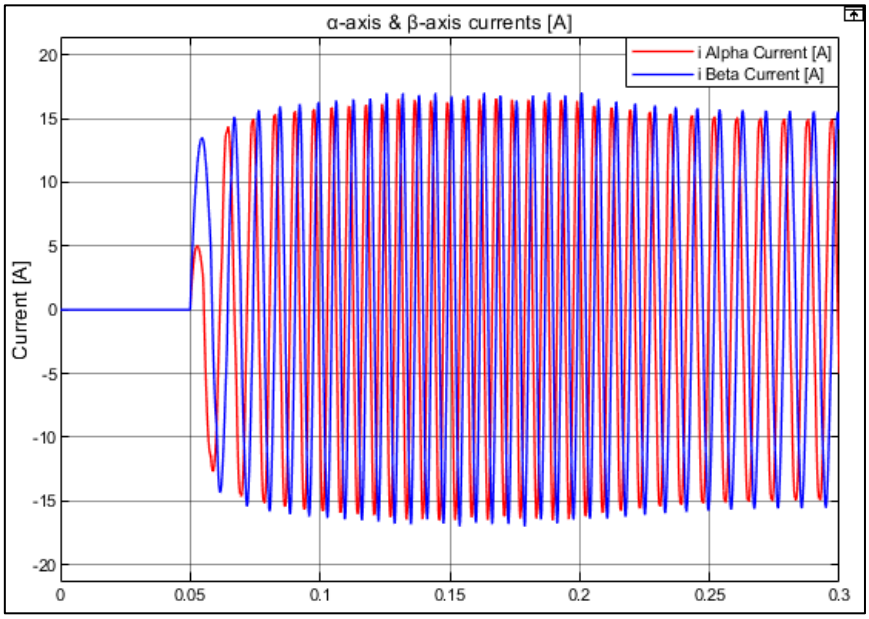

Figure 5.4 Sinusoidal i_α *and* i_β

As time progresses, the value of (i_α) and (i_β) changes sinusoidally as presented and their phase relation causes the plot to trace out as a circle. In an IPMSM under steady state, the stator currents are sinusoidal in nature with a phase difference of 120 degrees between the three phases. When these currents are transformed into the (α, β) stationary reference frame, the result is two sinusoidal currents, where the leading current is 90 degrees in front of the second one. This is the phase equivalent of the original 3-phase current which typically represents the rotating nature of the electromagnetic field in the motor. It is also evident that the magnitude of this current vector changes as the controller tries to regulate the motor.

5.4 Reference Speed and Shaft speed

The result presented in [Figure 5.5] shows the implementation of PI (Proportional Integral) controller. The result shows that the actual motor speed accurately followed the reference speed, indicating the effective performance of the PI controller along with the DTC strategy. The reference input for the PI controller was the desired speed of the motor. The output of the controller is compared with the electromagnetic torque of the IPMSM to generate an error signal for the torque hysteresis controller as illustrated in [Figure 3.10]. The torque hysteresis controller then determines the appropriate voltage vector that needs to be applied to the motor to minimize this error. The successful speed tracking validates the effectiveness of the control strategy in managing the performance of the IPMSM. A drop in speed can be witnessed at 0.2 seconds due to the application of load torque on the motor.

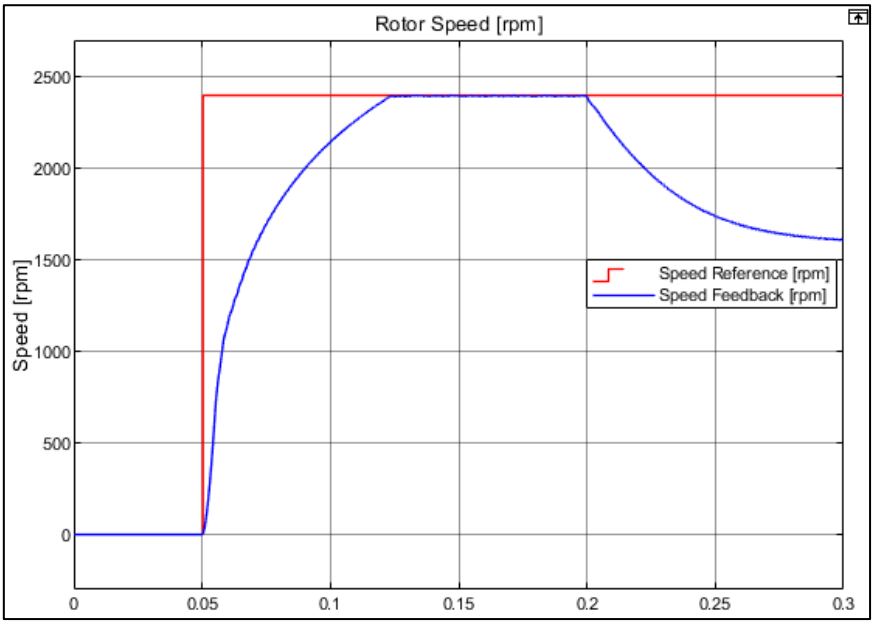

Figure 5.5 Reference speed Vs Rotor Shaft speed

5.5 Response to Load Torque

The result presented in [Figure 5.6] shows the response of the controller to load torque. An additional complexity was added by introducing a variable load torque into the

model after 0.2 seconds. This shows the system response to dynamically changing load conditions. The plot shows that the electromagnetic torque effectively tracked the reference load torque which indicates that the strategy was successful in maintaining control under variable load conditions. Once the desired reference speed is achieved, a drop in torque is observed which shows the reduction in output power once the set speed is reached. This algins with the expected behavior of a tuned PI controller. However, it is evident that the torque produced has a lot of ripples. This is an expected behavior of this control strategy. The simulation employed in this thesis applies the traditional DTC, leading to a noticeable amount of torque ripples. It is worth noting that DTC, in its standalone form, is not commonly utilized in controlling an IPMSM for an electric vehicle. It is typically combined with other advanced control methods like MPC and SVM. The aim of this combination is to effectively minimize the torque ripples, while still preserving the rapid dynamic response that the DTC control scheme is acclaimed for.

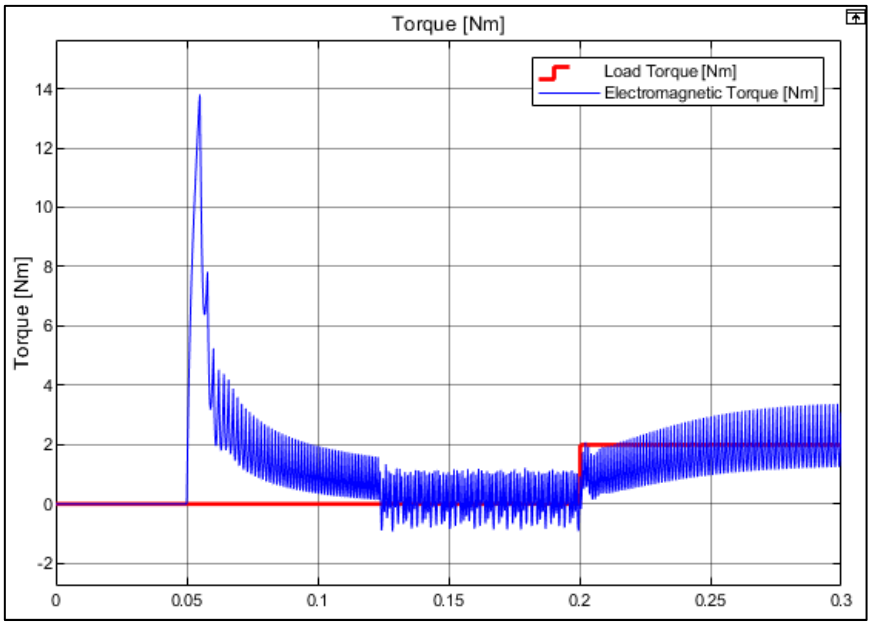

Figure 5.6 Reference Load torque Vs Electromagnetic torque

6 Discussion

The presence of multiple concentric hexagonal loops is indicative of the controller's constant regulation of motor torque, keeping the stator flux within the hysteresis band. However, it is important to note that the shape can vary based on the motor and inverter parameters, control strategies, modulation scheme, and other factors. It may not always be a perfect hexagon owing to the complexities involved in the operation and control of IPMSM.

The magnitude of the current vector varying as the controller regulates the motor provides an important insight into how effectively the controller maintains the motor's performance. It should be noted that in practical situations, these currents may not be perfectly sinusoidal due to several factors. A few of them are switching harmonics, dead time effects inside the inverters, non-ideal effects in the power transistors, distortions due to control loop discretization of control equations and machine non-idealities like changes in load and temperature variations.

The results affirm that the PI controller's response and the DTC strategy were successful in maintaining an accurate motor speed that tracked the reference speed. While tuning, the output of the PI controller is saturated between the minimum and maximum values of the torque that could be handled by the motor to prevent damages when the controller is compromised.

The presence of torque ripples suggests the need for further refinement in the control strategy. Future research might focus on the minimization of these torque ripples by exploring more switching algorithm like SVM or an entirely different control strategy like FOC. In addition to that, the control strategy could be further tested under different load conditions. The performance of the controller could also be further optimized by fine tuning the PI controller.

7 Conclusion

In conclusion, the study performed offers substantial evidence of the potential applications and effectiveness of the DTC method for controlling IPMSM. The 3-phase inverter demonstrates optimal performance in generating active voltage vectors using its characteristic hexagonal switching pattern. The role of DTC in ensuring the maintenance of stator flux and torque within the specified hysteresis bands is verified which further validates the theoretical principles discussed in the preceding chapters.

Furthermore, the magnitude and length of the stator flux vector is dependent on the motor load and command signal. The transformation of stator currents in the (α, β) stationary reference reveals the sinusoidal characteristics of these currents. The circular plot generated by the phase relation between (i_α) and (i_β) current confirms the motor's constant torque-level operation which is a key feature of an IPMSM.

The introduction of PI controller supports the DTC method by enabling a more precise speed control. A combination of controller and the switching strategy demonstrates a successful performance management with the actual motor speed closely following the reference speed. Moreover, the response of the controller to load torque depicts the ability of the controller to adjust the speed under changing load conditions and restrict the speed based on the physical limitation of the motor. However, the presence of torque ripples sets the stage for further refinement and optimization.

While the study validates the effectiveness of combined DTC and PI control strategy, it also indicates potential areas of improvements. Exploring advanced control techniques such as SVM, MPC, fuzzy logic control and neural networks could further minimize torque ripple and enhance system performance. Fine-tuning of the PI controller and switching algorithm could also prove beneficial. It is also recommended to perform further tests under dynamically varied load conditions to validate the robustness and adaptability of the control strategy. A future recommendation would be to conduct a real-time validation of the Simulink model by connecting it to an actual IPMSM to further establish the accuracy and effectiveness.

While this thesis provides valuable insights into the use of DTC control in IPMSM operation, it is important to acknowledge that it only explores a small fragment in the realm of motor control strategies. It is my sincere hope that this work sparks further interests and motivates future research in this field.

References

[1]. D. Swierczynski and M. P. Kazmierkowski, "Direct torque control of permanent magnet synchronous motor (PMSM) using space vector modulation (DTC-SVM)-simulation and experimental results," in *IEEE 2002 28th Annual Conference of the Industrial Electronics Society*. IECON 02, Seville, pp. 751-755 vol.1, Spain, 2002.

[2]. Krause, P. C., Wasynczuk, O., & Sudhoff, S. D, "Analysis of Electric Machinery and Drive Systems," Hoboken, NJ, USA: IEEE Press and John Wiley & Sons, Inc. 2013, ch. 12, pp. 485–500.

[3]. I. Takahashi and T. Noguchi, "A New Quick-Response and High-Efficiency Control Strategy of an Induction Motor," in *IEEE Transactions on Industry Applications*, vol. IA-22, no. 5, pp. 820-827, Sept. 1986.

[4]. D. Casadei, F. Profumo, G. Serra and A. Tani, "FOC and DTC: two viable schemes for induction motors torque control," in *IEEE Transactions on Power Electronics*, vol. 17, no. 5, pp. 779-787, Sept. 2002.

[5]. D. W. Novotny and T. A. Lipo, "Vector Control and Dynamics of AC Drives," New York, NY, USA: Oxford University Press, 1996, ch. 5, pp. 18-30, 73-80, 200–250.

[6]. C. J. O'Rourke, M. M. Qasim, M. R. Overlin and J. L. Kirtley, "A Geometric Interpretation of Reference Frames and Transformations: dq0, Clarke, and Park," in *IEEE Transactions on Energy Conversion*, vol. 34, no. 4, pp. 2070-2083, Dec. 2019.

[7]. R. Krishnan, "Electric Motor Drives: Modeling, Analysis, and Control," Upper Saddle River, NJ, USA: Prentice Hall, 2001, ch. 9, pp. 415-420, 513–530.

[8]. V. Biyani, J. R, T. E. T. A, S. S. V. S and P. K. P, "Comparative Study of Different Control Strategies in Permanent Magnet Synchronous Motor Drives," in *2021 IEEE 5th International Conference on Condition Assessment Techniques in Electrical Systems* (CATCON), Kozhikode, India, pp. 275-281, Dec. 2021.

[9]. L. Zhong, M. F. Rahman, W. Y. Hu and K. W. Lim, "Analysis of direct torque control in permanent magnet synchronous motor drives," in *IEEE Transactions on Power Electronics*, vol. 12, no. 3, pp. 528-536, May 1997.

[10]. S. A. R. Kashif, M. A. Saqib and M. ul Hassan, "Direct-torque control of a PMSM using four-switch three-phase inverter," in *IEEE 23rd International Symposium on Industrial Electronics (ISIE)*, Istanbul, Turkey, pp. 795-799, 2014.